

To what extent is the distribution of *Z. noltii* in South and West Wales changing?



Laura Pratt
Biology

Leanne Cullen-Unsworth and Benjamin Jones
Project Seagrass, Sustainable Places Research Institute
Word Count: 6647

Reflection of my placement

Abstract

This study focuses on the distribution of *Zostera noltii* in South and West Wales for which detailed information on the spatial and temporal variations in the seagrass distribution is sparse, despite being ecologically important. An effective monitoring method is there needed to quantify *Z. noltii* populations. The aim of this study was to provide a fine-scale assessment into the historical and current known distributions of *Z. noltii* and the magnitude of expansion/regression observed. Developing accurate maps of seagrass extent presents challenges including variable spatial distributions across a meadow, unfirm substrata and changes in water clarity. Given these challenges this research utilised a range of assessment methods and examined the potential use of a UAV (Unmanned Aerial Vehicle) for assessing seagrass distribution. The extent, health, and resilience of *Z. noltii* were assessed throughout South Wales and data compared against historical distributions. The outcomes showed the current spatial distribution of *Z. noltii*, covering a known area of 73.3ha, with an overall estimated expansion of $2.1\% \text{yr}^{-1} \pm 20.8$. Sites in Pembrokeshire such as West Williamson displayed a significantly higher seagrass condition with increased coverage, shoot density and canopy height values observed. However, sites in Glamorgan mostly on Llanrhidian Sands displayed a poorer *Z. noltii* health and signs of regression. In many of the locations where *Z. noltii* had historically been recorded it was no longer present, most likely due to extensive anthropogenic impacts.

Key words: *Zostera noltii*, UAV, remote sensing, Wales, Spatial heterogeneity

Table of Contents

	<i>Page number</i>
List of Figures.....	6
List of Tables.....	8
1.0 Introduction.....	9
1.1 <i>Z. noltii</i> status.....	11
1.2 <i>Z. noltii</i> monitoring.....	11
1.3 Unmanned aerial vehicles (UAVs) in <i>Z. noltii</i> monitoring.....	12
1.4 Aims and Objectives.....	13
2.0 Materials and Methods.....	15
2.1 Study sites.....	15
2.2 Mapping of the intertidal <i>Z. noltii</i> meadow boundary.....	18
2.3 Drone Based data collection.....	18
2.4 Morphological measurements.....	22
2.5 Seed coring.....	23
2.6 Data Analysis.....	24
3.0 Results.....	26
3.1 <i>Z. noltii</i> extent.....	26
3.2 Drone analysis.....	32
3.3 Seagrass Morphometrics.....	40
3.4 Historical change in <i>Z. noltii</i> morphometrics.....	43
3.5 Multivariate analysis of morphometric variables.....	44
3.6 <i>Zostera</i> Condition Index.....	45
3.7 <i>Z. noltii</i> morphometrics vs NDVI.....	47
3.8 Core Analysis.....	47
3.9 Field observations.....	49
4.0 Discussion.....	51
4.1 Seagrass status and extent.....	51
4.2 Differences in <i>Z. noltii</i> spatial distribution.....	55
4.3 Affectability of drones as an alternative seagrass monitoring platform.....	56
4.4 <i>Z. noltii</i> future and conservation.....	58
4.5 Conclusion.....	59
5.0 Acknowledgments.....	59
6.0 References.....	60
Appendices.....	66

List of Figures

Page number

Figure 1 <i>Zostera noltii</i> submerged in surface water located at Penclacwydd.....	9
Figure 2 Geographical locations of <i>Z. noltii</i> (dwarf eelgrass) in Europe.....	10
Figure 3 Global decadal trends in seagrass extent, with sites either decreasing, increasing or displaying no change in the size of a meadow.....	11
Figure 4 Map of the seagrass study sites visited along the South and West Wales coastline. Orange indicates sites that have a historical record of <i>Z. noltii</i> and green indicates sites that have been predicted to have suitable conditions for <i>Zostera</i> growth.....	16
Figure 5 Example flight path of 3DR Solo at Garren Pill, superimposed on orthomosaic generated on Photoscan 1.2.0. Waypointed routes were plotted using Mission Planner and flown using pixhawk autopilot.....	20
Figure 6 Example of overlapping images and computed camera positions recorded at A) Pwllcrochan and B) Garren Pill, C) fine- scale analysis at Angle Bay and D) lower altitude flight at Garren Pill, 2016.....	20
Figure 7 Steps used to create a three-dimensional model in Agisoft PhotoScan Professional.....	21
Figure 8 The process of coring; 1) Cores taken randomly with a standard PVC seed corer (50mm diameter x 250mm long) and cap, pushed approximately 10cm deep in the sediment; 2) Sediment placed in stainless steel sieve (1-2mm mesh); 3) Sieved sediment using a little water and 4) Analysis of core content.....	24
Figure 9 Differences in the area of seagrass recorded by 1) using a handheld GPS and 2) using transects, to assess different forms methodologies in monitoring larger <i>Z. noltii</i> meadows (A, Angle Bay and B, Penclacwydd).....	28
Figure 10 Non-linear regression model that can be used to predict the current <i>Z. noltii</i> extent based on historical (<2016) distributions.....	29
Figure 11 Evolution of the spatial distribution of <i>Z. noltii</i> from 2013 to 2016, at sites showing signs of regression.....	30
Figure 12 Evolution of the spatial distribution of <i>Z. noltii</i> from 2013 to 2016, at sites showing signs of expansion.....	31
Figure 13 Differences in the quality of the aerial data recorded at Garren Pill, July 2016, on a customized 3DR Solo, flown at 15m using; A) RICOH GR II consumer grade compact camera, B) modified Xiaomi Yi Action Camera (RGB) and C) modified Xiaomi Yi Action Camera (NIR/Blue filtered).....	33
Figure 124 Differences in the area of <i>Z. noltii</i> at A) Pwllcrochan and B) Garron Pill, recorded using Garmin GPSmap 62 and forms of classification of the UAV data carried out on ArcMap 10.2.2.....	34
Figure 15 Unsupervised ISO Cluster classification of true-colour mosaics at both A) Pwllcrochan (30m) and B) Garren Pill (50m).....	35
Figure 13 Supervised Maximum Likelihood image classification (MLC) of true-colour mosaics at both A) Pwllcrochan and B) Garren Pill.....	36
Figure 17 The process of manual classification used to assess <i>Z. noltii</i> boundaries at Pwllcrochan.....	37

Figure 18 Relative NDVI map generated from true-colour and NIR imagery at taken using a modified Xiaomi Yi Action Camera, at Garron Pill, July 2016.....	38
Figure 19 Differences in the NDVI (Means \pm 95%CI) calculated for the different spectral classifications of the intertidal aerial data.....	39
Figure 20 Mean (\pm 95%CI) <i>Z. noltii</i> cover, shoot density, leaf length, leaf width, epiphyte cover and algae cover across all 10 study sites. Green indicates values that were recorded in a <i>Z. noltii</i> meadow that displayed signs of expansion, yellow no detectable change in the meadow size and red, a <i>Z. noltii</i> meadow with observed regression correlations in the area.....	42
Figure 21 Changes in the average <i>Z. noltii</i> cover (Means \pm 95CI) and mean canopy height (mm) observed at Angle Bay from 1996 to 2000. Blue indicates historical values obtained from Hodges and Howe, 2007, yellow, Bunker, 2008, and green, Duggan-Edwards and Brazier, 2015, with the shoot density values obtained from the same data source.....	43
Figure 22 Principal component analysis (PCA) of seagrass characteristics from 10 different study sites, spread along the South and West Wales coastline.....	45
Figure 23 Non-linear regression model, estimating the relationship between the Normalised Difference Vegetation Index (NDVI) and dominant <i>Z. noltii</i> habitat characteristics. Red represents changes in <i>Z. noltii</i> cover, yellow shoot density and green canopy height.....	48
Figure 24 Mean (\pm 95%CI) <i>Z. noltii</i> seed density (m ²) at both sites where seagrass was present (green) and sites where <i>Zostera spp</i> were absent (red).....	49
Figure 25 Area of intensive bait digging to the north of the intertidal <i>Z. noltii</i> bed in Angle Bay. Source: authors own, 2016.....	50
Figure 26 Opportunistic macroalgae observed at West Williamson, from extensive algae cover of the <i>Z. noltii</i> bed. Source: authors own, 2016.....	50
Figure 27 Observed <i>Z. noltii</i> bleaching at Angle Bay, where the causality is unknown. Source: authors own, 2016.....	50
Figure 28 Tractor marks observed at <i>Zostera</i> meadow in Porthdinllaen.....	54
Figure 29 Aerial data recorded at Pwllcrochan, July 2016, where strong winds led to the model (DJI Phantom 3 Professional) blocking part of the photograph.....	57

List of Tables

	<i>Page number</i>
Table 1 Physical factors that influence <i>Z. noltii</i> growth and seagrass distribution.....	10
Table 2 Review of previous forms of remote sensing that have been used to monitor and map global seagrass populations.....	14
Table 3 Range of data sources used to identify historical locations of <i>Z. noltii</i> found in South and West Wales.....	15
Table 4 Geographical location of the study sites, historical and current record of <i>Z. noltii</i> presence and initial anthropogenic threats observed nearby (within a 500m radius) the <i>Z. noltii</i> meadows.....	17
Table 5 Differences in the technical specifications between the three unmanned aerial vehicles (UAV) models used in this study.....	19
Table 6 Parameters used in the steps to generate orthomosaics and DEM's from aerial data in Agisoft Photoscan Pro 1.2.0.....	22
Table 7 Surface area of <i>Z. noltii</i> at the 10 study sites where seagrass was found to be present along the South and West Wales coastline.....	27
Table 8 Differences in the time spent using a handheld GPS and light weight UAV to map the spatial and temporal distribution of <i>Z. noltii</i> meadows.....	32
Table 9 Seagrass parameters recorded at 13 of the locations where <i>Z. noltii</i> was found to be present along the South and West Wales coastline.....	41
Table 10 PCA results of 10 <i>Z. noltii</i> sites sampled along the South and West Wales coastline.....	44
Table 11 Report card for the seagrass condition for <i>Z. noltii</i> meadows in the South and West Wales region (March – July 2016). <i>Zostera</i> condition score and index were calculated using seagrass cover, shoot density and canopy height. Dark green indicates very good condition, green is good condition, yellow is moderate condition, orange medium poor condition and red very poor condition.....	46
Table 12 European <i>Z. noltii</i> meadows, where expansion of the extent has been recorded in previous literature.....	51
Table 13 Possible explanatory mechanisms for the expansion of <i>Z. noltii</i> at specific study sites (PE, AB, PW, PD and WW) from 2004.....	53
Table 14 Estimates of <i>Z.noltii</i> seed density recorded in previous literature.....	55
Table 15 The decision rules used to classify <i>Z. noltii</i> beds that had previously been remotely sensed with SPOT multispectral images.....	58

1.0 Introduction

Seagrass are marine flowering plants (angiosperms) that form extensive beds in shallow and sheltered coastal lagoons and estuaries, providing an essential habitat for many coastal species (Short *et al.* 2011). In the UK two species of seagrass are recognised; *Zostera marina* (eelgrass) and *Zostera noltii* (dwarf eelgrass). *Z. noltii* (Figure 1) is an intertidal species rarely found past the low tide mark (Stace 1997), with its distribution extending along the Atlantic coasts ranging from south Mauritania (Cunha and Araujo 2009) to the southern fjords of Norway (den Hartog 1970)(Figure 2). It is commonly found adjacent to saltmarsh communities and relies on specific environmental conditions in order to grow and survive (Table 1). *Z. noltii* is ecologically and economically important, acting as an ecosystem engineer by attenuating waves (Paul and Amos 2011) and encouraging the accretion of sediments. The roots and rhizomes of the plant help to stabilise the substratum, improving water quality and thus creating a dynamic favourable habitat that displays higher levels of biodiversity than other unvegetated areas (Bertelli and Unsworth 2014). Polte (2005) displayed how *Z. noltii* meadows function as nursery and extended juvenile habitats for epibenthos and provide a source of food to wildfowl including *Branta bernicla* (Brent goose), *Anas Penelope* (Eurasian wigeon) and *Cymus olor* (Mute Swan) (Davison and Hughes 1998). Furthermore, seagrass meadows act as carbon sinks, accounting for 10-18% of the total oceanic carbon burial despite only covering 0.1% of the world's ocean floor (Mcleod *et al.* 2011).



Figure 1 *Zostera noltii* submerged in surface water located at Penlacwydd, Carmarthenshire. Source: authors own, 2016.



Figure 2 Geographical locations of *Z. noltii* (dwarf eelgrass) in Europe, possessing a smaller range than other *Zostera* spp. Source: Borum and Greve, 2004.

Table 2 Physical factors that influence *Z. noltii* growth and seagrass distribution.

Environmental Factor	Optimum <i>Z. noltii</i> Conditions
Depth and Light availability	Like all plants <i>Z. noltii</i> requires light to photosynthesis. The intertidal species is found at a range of depths from 0-10m (Short et al. 2011) and tends to survive in shallower, high light intensities than <i>Z. marina</i> due to its small rhizomes that limit the plant's ability to store carbohydrates. <i>Z. noltii</i> has also displayed signs that it is able to adapt to differences in water depth by adjusting its growing behaviour. In shallow waters it produced dense but short meadows, whereas longer leaves are often found at deeper sites (REFERENCE).
Sediment	<i>Z. noltii</i> grows on sandy to muddy substrata (Davison and Hughes 1998). Unlike other <i>Zostera</i> spp, <i>Z. noltii</i> prefers finer-textured sediments that provide higher fertility, allow rhizome elongation and have greater levels of anoxia. Fine soft sediments are often found in sheltered, low energy environments that remain partly submerged to stop the roots from drying out.
Temperature	<i>Z. noltii</i> can survive at a range of temperatures from 7°C to 23°C and the optimum temperature for growth and germination appears to be between 10°C -15°C (Davison and Hughes 1998). The average temperatures observed in Wales (winter temperatures around 8°C and summer highs around 17°C) are within this range therefore temperature is unlikely to be the limiting factor if <i>Z. noltii</i> distribution.
Salinity	<i>Z. noltii</i> is a euryhaline species (Paul 2011), that can tolerate high salinities (15-30‰) but also survive in brackish conditions down to salinities less than 5‰ (Charpentier et al. 2005). However, <i>Z. noltii</i> generally prefers lower salinity conditions for germination (optimum 1.0‰ salinity) and therefore freshwater run off can be said to influence the distribution of <i>Z. noltii</i> (Hootsmans et al. 1987)
Disturbance/Exposure	<i>Z. noltii</i> like other seagrass species, requires a sheltered environment to survive (Davison and Hughes 1998).

1.1 *Z. noltii* status

Seagrass species are globally in decline (Green and Short 2003), significantly reducing since the 1970s (Figure 3). *Z. noltii* is listed in the Least Concern category of the International Union for the Conservation of Nature's (IUCN) Red List of Threatened Species, primarily due to its large range size, however *Z. noltii* has displayed declining population trends (Short *et al.* 2010). *Zostera* communities in Wales are listed as a UK Biodiversity Action Plan habitat (Maddock 2011), with declines in the seagrass abundance thought to be caused by a variety of factors including *Zostera* wasting disease, climate change (reducing the metabolism of the plant) and eutrophication from anthropogenic threats (Jones and Unsworth 2016). It is therefore important to map and understand the current distribution of *Z. noltii* meadows, to help monitor and safeguard the future of this marine habitat. Seagrass species are also considered indicators of water quality and health, due to their susceptibility to changes in environmental factors (Pergent-Martini and Pergent 2000; Bhattacharya *et al.* 2003), with degraded habitats influencing their effectiveness as ecosystem stabilisers (Uhrin and Townsend 2016). Therefore, monitoring the condition of *Z. noltii* populations is vital.

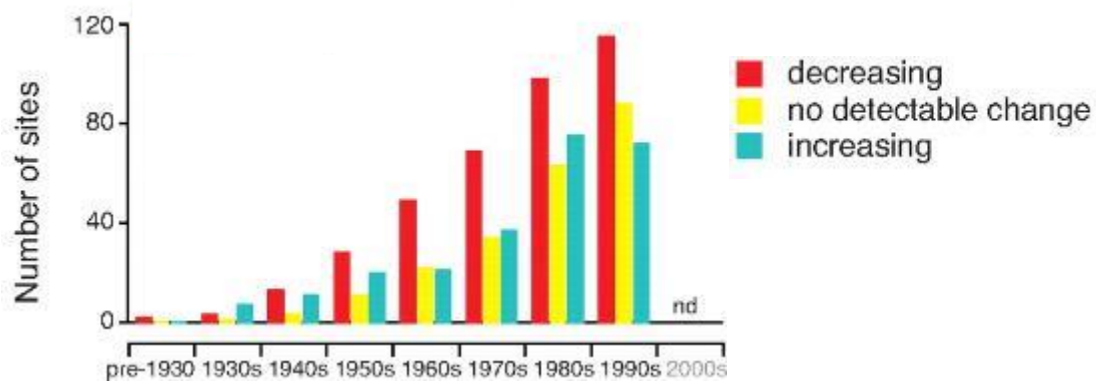


Figure 3 Global decadal trends in seagrass extent, with sites either decreasing, increasing or displaying no change in the size of a meadow. Adapted from Waycott *et al.* (2009).

1.1 *Z. noltii* status

There exists limited detailed information about the current distribution of *Z. noltii* in South and West Wales as mapping of *Zostera* meadows is inherently difficult due to factors such as unfirm substrata, cold temperatures and high winds/ground

swell/wind swell causing changes in water clarity leading to poor visibility. Historical records of *Z. noltii* are sparse and often incomplete with the volume, accuracy and reliability of data taken from the marine ecosystem being significantly less than that of terrestrial environments (Carr *et al.* 2003). The extent of the data is often limited, only focusing on well-known locations and many of the records only display habitat occurrence through point formats that do not represent the spatial and temporal changes in the dynamic *Z. noltii* habitat. Many of the historical records of *Z. noltii* were falsely identified as *Z. angustifolia*, the phenotypic variation of *Z. marina*. This previous taxonomic confusion, in addition to differing nomenclature (Box 1.0), has led to a severe lack of understanding and underestimate of *Z. noltii* populations in Wales (Kay 1998). Comprehensive strategies for both the mapping and inventorying changes in the *Z. noltii* habitats are needed; to clarify the current distribution of the species and to derive the biophysical properties of the meadows (Armstrong 1993; Koedsin *et al.* 2016) that have not been previously recorded. Predictive habitat distribution models are also increasingly being used to map the species location where there is a lack of resources (Grech and Coles 2010; Brown 2015). An accurate GIS map of the *Z. noltii* meadows in South and West Wales could therefore help in the development and to quantify results of future models.

Box 1.0 Scientific nomenclature of *Z. noltii*

For the purpose of this study dwarf eelgrass is referred to as *Z. noltii* to avoid confusion with previous scientific literature. However, on the World register of marine species *Zostera noltii* is not accepted and instead recorded as *Z. noltei*. There is also current discussion as to whether dwarf eelgrass may in fact be of a separate genus, *Nanozostera noltii* (Coyer *et al.* 2013).

1.4 Unmanned aerial vehicles (UAVs) in *Z. noltii* monitoring

Remote sensing and manual delineation of marine ecosystems through photointerpretation is becoming widely used by researchers, as it enables scientists to map and assess fragile marine environments without disturbing them (McEvoy *et al.* 2016). Previous studies have focused on obtaining data from larger remote-sensing instruments that are not designed for detailed biological monitoring (Anderson and Gaston 2013) (Table 2). However, developments in the use of UAV technology have meant that using remote sensing has become a more accessible

tool for smaller teams and projects, with such developments providing the platform for UAVs to be used as effective mapping tools for seagrass meadows. Meadows often have varying percentage covers, from extensive, and continuous to aggregations of patchy mounds, which are difficult to include in mapped polygon data. The use of aerial data for remote sensing allows unvegetated parts of a meadow to be mapped within a polygon, providing an accurate and comprehensive map of the spatial distribution of an individual meadow compared to point and transect based surveys (Lyons *et al.* 2011; Koedsin *et al.* 2016). The use of drone technology can also provide an alternative in areas where the water is too deep or conditions too turbid for satellite remote sensing. However, some seagrass mapping results have reveal low accuracy in some of the biophysical measurements compared to field observations, with sparse areas often being misclassified (Knudby and Nordlund 2011). The use of neo-infrared cameras on a UAV offers potential solutions to misclassification (Barille *et al.* 2009). Assessing the ability of this form of remote sensing to map intertidal *Z. noltii* populations will help to provide valuable data and evidence in the development of novel drone-based approaches.

1.5 Aims and Objectives

This study describes an assessment of the distribution and status of *Z. noltii* in South and West Wales.

The aims are to;

- 1) Identify changes in the physical location of *Z. noltii* populations compared to historical distributions.
- 2) Trial photographic mapping at specific sites and assess the ability of a drone as an effective *Z. noltii* mapping tool.

Outcomes of the study were to generate a series of vector data over a wide spatial scale across South and West Wales and look at how the knowledge of this species distribution can help in its conservation.

Table 2 Review of previous forms of remote sensing that have been used to monitor and map global seagrass populations. Adapted from Hossain et al, 2015.

Aerial data platform	Examples	Published Studies
Hyperspectral Satellite	Hyperion	Lee et al. (2005), Pu and Bell (2013), Pu et al. (2012)
Multispectral Satellite (High spectral resolution)	IKONOS, Quickbird, WorldView2	Maeder et al. (2002), Mumby and Edwards (2002), Hochberg, Andrefouet and Tyler (2003), Dekker, Brando and Anstee (2005), Purkis and Riegl (2005), Wolter, Johnston and Niemi (2005), Fornes et al. (2006), Mishra et al. (2006), Habeeb et al. (2007), Karpouzli and Malthus (2007), Phinn et al. (2008), Sagawa et al. (2008), Yuan and Zhang (2008), Dingtian (2009), Dogan, Akyerk, and Belioglu (2009), Howari et al. (2009), Urbanski, Mazur and Janas (2009), Yang and Yang (2009), Amran (2010), Knudby and Nordlund (2011), Lyons, Phinn, and Roelfsema (2011), Liew and Chang (2012), Hamylton, Hagan, and Doak (2012), Phinn, Roelfsema, and Mumby, (2012), Baumstark et al. (2013), Borfecchia et al. (2013), Lee, Weidermann, and Arnone (2013), Roelfsema, Phinn et al. (2013), Tamondong et al. (2013), Roelfsema et al. (2014),
Multispectral Satellite (Medium spectral resolution)	Landsat MSS, Thematic Mapper, Enhanced Thematic Mapper+, ALI, China Brazil Earth Resources Satellite, Satellite Pour l'Observation de la Terre, Advanced Land Observing Satellite, Advanced Spaceborne Thermal Emission and Reflection Radiometer	Ackleson and Klemas (1987), Lennon and Luck (1989), Khan, Fadlallah, and Al-Hinai (1992), Armstrong (1993), Mumby et al. (1997), Ferguson and Korfmacher (1997), Andrefouet et al. (2001), Chauvard, Bouchon, and Maniere (2001), Mumby and Edwards (2002), Purkis et al. (2002), Bouvet, Ferraris, and Andrefouet (2003), Call, Hardy, and Wallin (2003), Lunden and Gullstrom (2003), Schweizer, Armstrong and Posada (2005), Pasqualini et al. (2005), Gullstrom et al. (2006), Shapiro and Rohmann (2006), Vanderstraete, Goossens, and Ghabour (2006), Cho (2007), Lauer and Aswani (2008), Matarrese et al. (2008), Phinn et al. (2008), Wabnitz et al. (2008), Howari et al. (2009), Roelfsema et al. (2009), Yang and Yang (2009), Barille et al. (2010), Knudby et al. (2010), Zhang (2011), Lyons, Phinn and Roelfsema (2012), Meyer and Pu (2012), Pu et al. (2012), Chen et al. (2013), Pu and Bell (2013), Roelfsema, Kovacs, et al. (2013), Torres-Pulliza et al. (2013), Wicaksono and Hafizt (2013), Knudby et al. (2014)
Multispectral Satellite (Low spectral resolution)	Moderate Resolution Imaging Spectrometer, Medium Resolution Imaging Spectrometer	Kutser, Vahtmae, and Martin (2006), Saulquin et al. (2013), Petus et al. (2014)
Aircraft (Laser)	Lidar	Wang and Philpot (2007), Chust et al (2008), Tulldahl and Wikstrom (2012)
Aircraft (Hyperspectral)	Compact Airborne Spectrographic Imager, HyMap	Mumby et al. (1997), Mumby and Edwards (2002), Habeeb et al. (2007), Peneva, Griffith, and Carter (2008), Phinn et al. (2008), Brando et al. (2009), Casal et al. (2013)
Aerial (Photograph)	AP, HR digital camera	Benton and Newman (1976), Larkum and West (1990), Orth, Moore, and Nowak (1990), Robins (1997), Chauvaud, Bouchon, and Maniere (1998), Kendrick, Eckersley, and Waler (1999), Kendrick et al (2000), Moore, Wilcox, and Orth (2000), Seddon, Connolly, and Edyvane (2000), Lathrop et al. (2001), Pasqualini et al (2001), Andrefouet et al. (2002), Cuevas-Jimenez, Ardisson and Condal (2002), Kendrick et al. (2002), Agostini et al (2003), Leriche et al. (2004), Meehan, Williams, and Watford (2005), Zharikov et al. (2005), Aswani and Lauer (2006), Hernandez-Cruz, Purkis, and Riegl (2006), Leriche et al. (2006), Habeeb et al. (2007), Holmes et al. (2007), Mount (2007), Mudoch et al. (2007), Reise and Kohlus (2008), Young et al (2008), Cunha and Santos (2009), Fletcher, Pulich, and Hardegree (2009), Andrade and Ferreira (2011), Cuttriss, Prince, and Castley (2013), Dolch, Duschbaum, and Reise (2013), Buttger, Nehls, and Stoddard (2014)
Boat (Acoustic)	Side scan sonar, SDES, MBES, Acoustic Doppler current profiler, Sediment Image Sonar	Hughes Clarke, Mayer and Wells (1996), Siccardi, Bozzano, and Bono (1997), Komatsu and Tatsukawa (1998), Pasqualini et al. (1998), McCarthy and Sabol (2000), Pasqualini et al. (2000), Sabol et al. (2002), Komatsu et al. (2003), Shono et al. (2004), Jordan et al. (2005), Riegl et al (2005), Siwabessy et al. (2006), Karpouzli and Malthus (2007), Ryan et al. (2007), Warren and Peterson (2007), Wilson et al. (2007), Lo Iacono et al. (2008), Sagawa et al. (2008), Lefebvre et al. (2009), Marsh and Brown (2009), Ahsan et al. (2010), Brooke, Creasey, and Sexton (2010), De Falco et al. (2010), Dekker et al. (2011), Descamp et al. (2011), Di Maida et al. (2011), Hamilton and Parnum (2011), Paul et al. (2011), Hasan, Ierodionou, and Laurenson (2012), Micallef et al. (2012), Sanchez-Carnero et al. (2012), Montefalcone et al. (2013), Munday, Moore, and Burczynski (2013)
Boat (Laser)	FILLS	Dierssen et al. (2003)

2.0 Materials and methods

2.1 Study sites

The Welsh coastline stretches 1680 miles (2740km) (WWF 2012), bordering the Irish Sea and Bristol Channel. *Z. noltii* populations in Glamorgan, Carmarthenshire and Pembrokeshire were assessed, and using all known historical data of seagrass coverage in the region sites were revisited to examine temporal change. Historical records were obtained from a range of sources (summarised in Table 3) and areas that have environmental parameters where *Z. noltii* has the potential to grow and thrive. Those sites suggested in Brown's (2015) potential distribution model were also sampled. Locations where records of *Z. noltii* consisted of leaves washed up on a beach were not used, as leaf litter can travel large distances (McMahon *et al.* 2014) and "cast up" does not necessarily indicate the presence of a nearby meadow (Kay 1998).

23 intertidal locations (Figure 4) along the South Wales coastline were assessed during March-July 2016 at low tide. Unfortunately, *Z. noltii* in the Pembroke River was unable to be included in the study. At each site, the presence or absence of *Z. noltii* was recorded and habitat data was collected in the field. Details on the anthropogenic impacts in the area were recorded (Table 4), to put the data in context, and identify threats that might influence *Z. noltii* distribution (Jones and Unsworth 2016).

Table 3 Range of data sources used to identify historical locations of *Z. noltii* found in South and West Wales.

Data Source	Data type
NRW (formally Countryside Council for Wales, CCW)	Reports, GIS layer, Point and Polygon shapefiles of <i>Z. noltii</i> presence, Global Positioning System (GPS) latitude/longitude with 10m error.
Botanical Society of Britain and Ireland	<i>Z. noltii</i> presence points only
(Kay Q, 1994)	Report summarizing data collection from county records and other key sources.

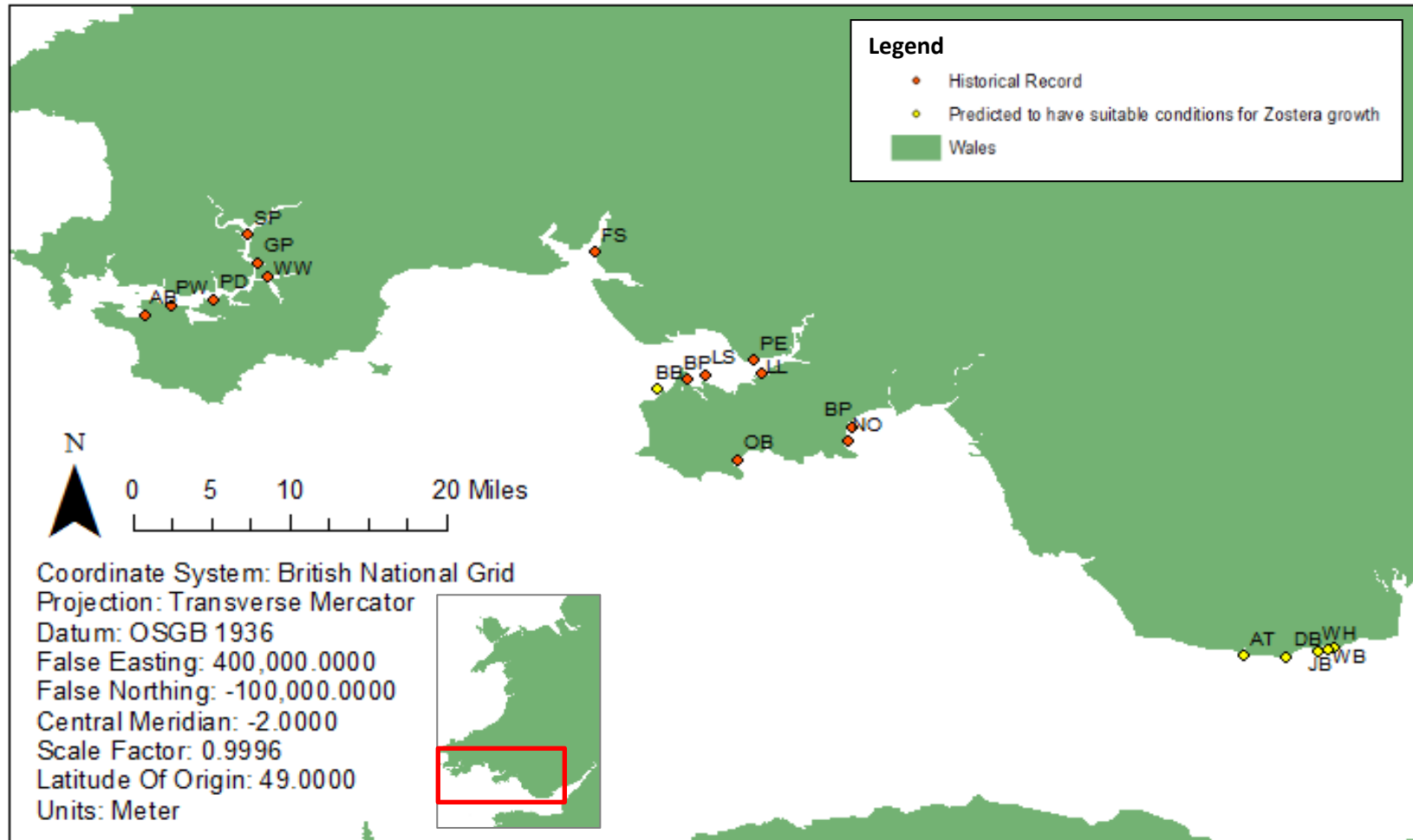


Figure 4 Map of the seagrass study sites visited along the South and West Wales coastline. Orange indicates sites that have a historical record of *Z. noltii* and green indicates sites that have been predicted to have suitable conditions for *Zostera* growth (Brown 2015). *Ruppia maritima* historical records were also found at Aberthaw lagoon, in addition to displaying suitable *Zostera* growth conditions. Source: L. Pratt, ArcMap 10.2.2, 2016.

Table 4 Geographical location of the study sites, historical and current record of *Z. noltii* presence and initial anthropogenic threats observed nearby (within a 500m radius) the *Z. noltii* meadows. Ranking of the anthropogenic threats indicated by colour; red (extremely high), orange (high), yellow (Adequete), green (low) and dark green (extremely low). Adapted from Jones (2014).

Site	Site Code	Coordinates	Date Visited	Most recent <i>Zostera</i> historical record	<i>Z. noltii</i> presence in 2016	Industry	Tourism	Agriculture	Catchment	Population	Anchoring	Permanent Mooring	Ranking of threats
Jackson Bay	JB	51°23'26.04"N 3°15'48.36"W	9 May 2016	-	Absent		X			X			2
Whitmore Bay	WB	51°23'18.14"N 3°16'25.71"W	9 May 2016	-	Absent		X			X			2
Watch House Bay	WH	51°23'17.77"N 3°17'19.26"W	10 May 2016	-	Absent		X			X			2
Dams Bay	DB	51°22'55.73"N 3°20'08.62"W	20 May 2016	-	Absent					X			1
Aberthaw	AT	51°22'54.17"N 3°23'04.31"W	12 April 2016	1998	Absent	X	X						2
Blackpill	BP	51°35'40.97"N 3°59'21.41"W	10 April 2016	1985-1995	Absent	X	X			X		X	4
Norton	NO	51°34'48.85"N 3°59'39.91"W	11 April 2016	1985-1995	Absent	X	X			X			3
Oxwich Bay	OB	51°33'33.88"N 4°09'18.32"W	6 May 2016	1974	Absent		X			X	X		3
Broughton Bay	BB	51°37'21.13"N 4°16'50.31"W	6 April 2016	1994	Absent		X			X			2
Burry Pill	BP	51°37'59.56"N 4°13'57.32"W	21 March 2016	2004	Present								0
Llanrhidian Sands	LS	51°38'01.79"N 4°11'21.24"W	24 June 2016	2013	Present			X					1
Llanmorlais	LL	51°38'36.87"N 4°07'33.01"W	23 April 2016	1916	Absent	X			X	X			3
Penclawydd	PE	51°39'18.66"N 4°08'21.50"W	23 March 2016	2013	Present	X	X		X	X			4
Ferryside	FS	51°45'20.35"N 4°22'38.72"W	4 May 2016	1947	Absent		X			X			2
Angle Bay	AB	51°40'46.64"N 5°02'43.59"W	12 March 2016	2013	Present	X			X	X			3
Pwllcrochan	PW	51°41'25.14"N 5°00'28.76"W	23 June 2016	2013	Present	X			X	X	X		4
Pembroke Dock	PD	51°41'47.83"N 4°56'45.01"W	6 June 2016	2013	Present	X	X		X	X	X	X	6
West Williamson	WW	51°43'12.86"N 4°51'50.51"W	8 July 2016	2013	Present		X	X		X		X	4
Garon Pill	GP	51°44'03.31"N 4°52'47.97"W	10 June 2016	2013	Present			X					1
Sprinkle Pill	SP	51°45'37.52"N 4°53'57.43"W	22 May 2016	2013	Present			X	X				2

2.2 Mapping of the intertidal *Z. noltii* meadow boundary

If *Z. noltii* was present and the meadow had a clear, definitive boundary, the boundary was mapped by walking around the meadow edge with a handheld GPS unit (Garmin GPSmap 62 and GPSmap 62stc) in tracking mode (accuracy error of approximately 1m). The data was then incorporated into the ArcGIS software by ESRI (Environmental Systems Resource Institute), specifically ArcMap 10.2, for geoprocessing using the British National Grid coordinate system. Single polygons (Duggan-Edwards and Brazier 2015) were generated, from which the area of the meadow was calculated and compared to the historical records. If any changes were observed the percentage of regression and expansion was calculated (Telesca *et al.* 2015). However, if the meadow was extremely large (>100km²) and patchy, with an inconsistent plant density (changing throughout the bed), transects were sampled perpendicular to the shoreline, starting where *Z. noltii* was present. Observers marked GPS waypoints every 50m and the presence/absence of *Z. noltii* along with the percentage cover was recorded. Transects were 100m apart, enabling an overall sampling grid to be created over a single bay and percentage cover was assessed by placing a 50cmx50cm stainless steel quadrat consistently in front of the right foot of the navigator, whilst walking along the area grid. Meadow boundaries were determined by continuing along the transects until three successive points indicated no presence of *Z. noltii* (Rasheed *et al.* 2003) and transects continued along the shore until *Z. noltii* was no longer found.

2.3 Drone Based data collection

Mapping the *Z. noltii* meadows on foot was only feasible in areas with relatively firm substrata, therefore this method could not be used in areas such as Garron Pill, where the substrate is soft mud (Bunker 2008). In these inaccessible areas a drone was used as a platform from which to collect photographs, which in turn could be stitched together to form a complete mosaic of a meadow. A DJIGlobal Phantom 3 Advanced UAV (Table 5) with a built-in Sony EXMOR1/2.3", was used in its autonomous flight mode to capture overlapping JPEG images (12 megapixels). It was flown along a transect so that captured images could be incorporated into a larger mosaic. It was flown using the DJI GO app for iPhone 5S controlled by a pilot and an observer, and prior to flight linear transects were plotted onsite, to avoid

any obstacles in the field. Multiple missions were conducted at fixed heights, to ensure the whole meadow was captured and to identify the optimum height at which *Z. noltii* can clearly be identified. To avoid sun glints effects, flights were also preferentially carried out early morning or late evening during cloudy weather, if compatible with low tides (Jaud *et al.* 2016). Aerial images were also taken on a customized 3DR solo and 3DR Y6, where a similar method was used to assess the use of the different models as environmental mapping tools. Aerial photographs were captured on with a twin set of modified Xiaomi Yi Action Cameras (both RGB and NIR/Blue filtered) and a RICOH GR II consumer grade compact camera where both RAW and JPEG images were captured to test the ability of the different cameras. The NIR/Blue filtered camera was also used to assess the spectral properties of seagrass related to the reflective part of the visible and infrared spectrum that cannot be observed through panchromatic photographs. The drones were flown using waypointed routes plotted using Mission Planner and flown using pixhawk autopilot (Figure 5). They were typically flown at a velocity of 5m/s in order to guarantee at least 50% overlap between the successive images (Figure 6)

Table 5 Differences in the technical specifications between the three UAV vehicles models used in this study. Source of the model images: authors own, 2016.



**DJI Global Phantom 3
Advanced UAV**



Customized 3DR Y6



Customized 3DR Solo

	DJI Global Phantom 3 Advanced UAV	Customized 3DR Y6	Customized 3DR Solo
Weight (including battery and propellers) (g)	1280	2500	1800
Max Speed	16m/s (ATTI mode/no wind)	10m/s	55mph (89 km/h)
Max Flight Time (minutess)	23	10	20

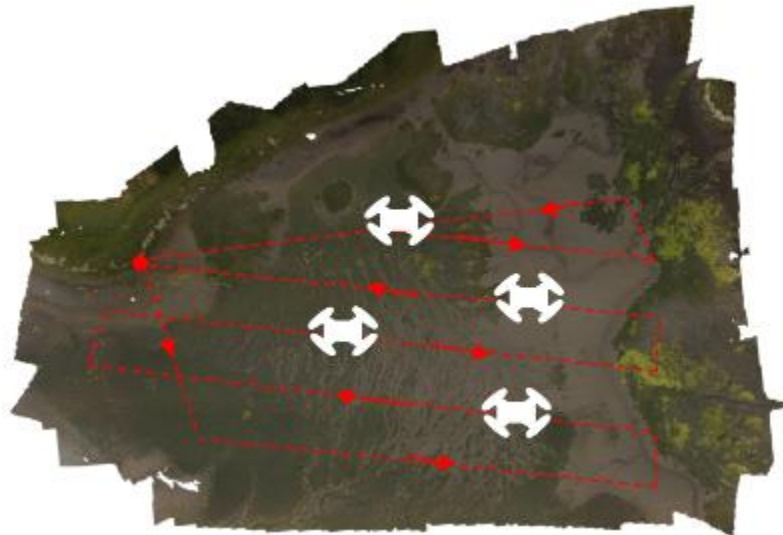


Figure 5 Example flight path of 3DR Solo at Garren Pill, superimposed on orthomosaic generated on Photoscan 1.2.0. Waypointed routes were plotted using Mission Planner and flown using pixhawk autopilot. using Source: L, Pratt, 2016.

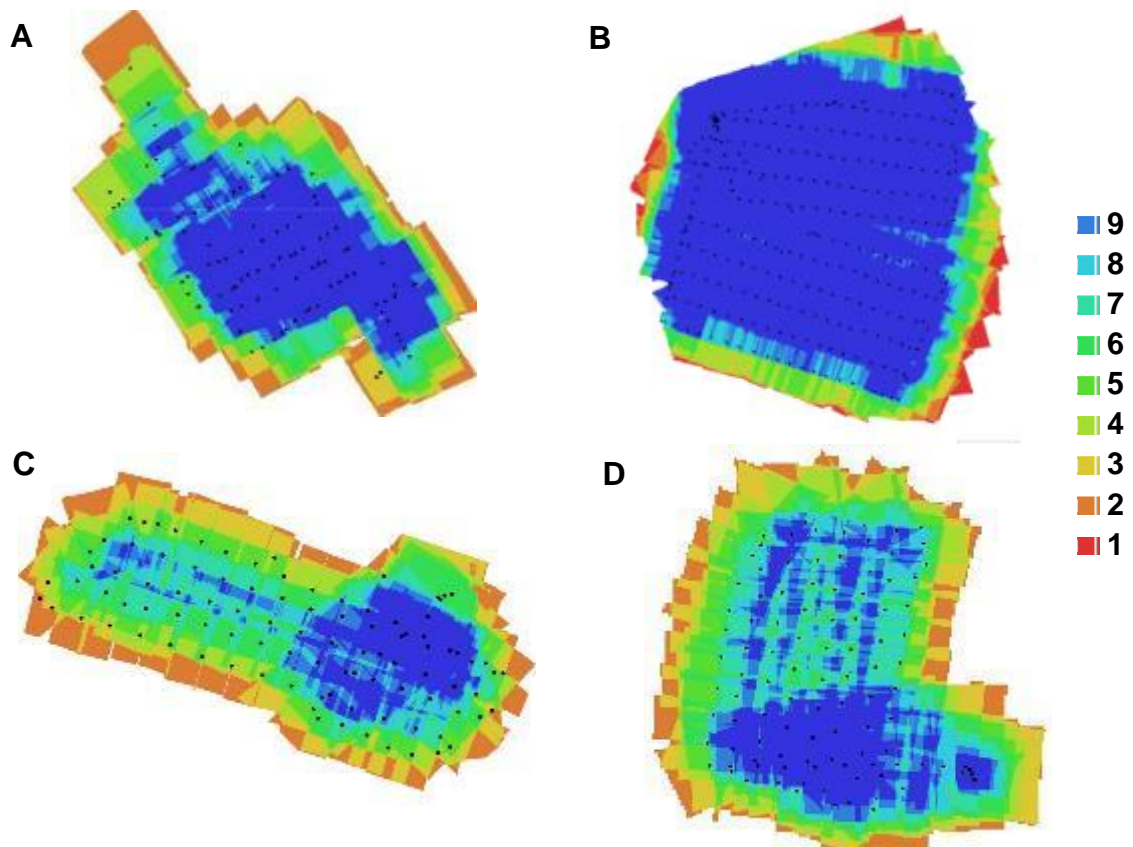
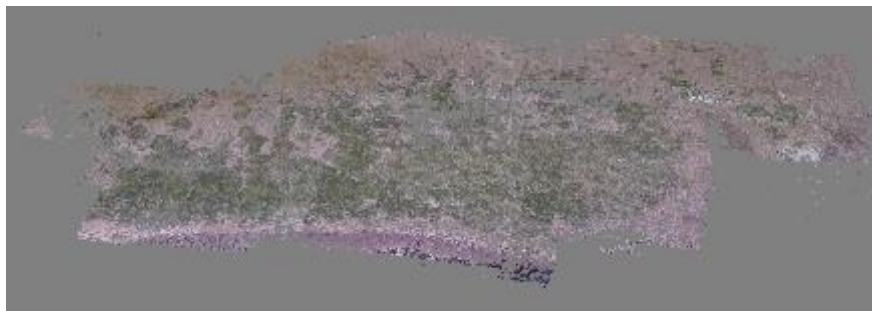


Figure 6 Example of overlapping images and computed camera positions recorded at A) Pwllcrochan and B) Garren Pill, C) fine- scale analysis at Angle Bay and D) lower altitude flight at Garren Pill, 2016. Higher levels of overlap were observed on the RICOH GR II consumer grade compact camera as oppose to the modified Xiaomi Yi Action Cameras (Appendix 1). Source: L, Pratt, 2016, using PhotoScan 1.2.0.

3D textured models were then generated from the digital images using the image processing software Agisoft PhotoScan Professional Version 1.2.0 (Agisoft 2015). The models were created off 3 major steps (Figure 7) (Casella *et al.* 2016; Ventura *et al.* 2016) using specific parameters (Table 6) and exported as georeferenced TIFFs (Tagged Image File Format) for further analysis. TIFFs were

Alignment of the photographs using *structure from motion* (SFM) to form a **point cloud** (Ullman 1979)



Polygonal **mesh** generated from dense multiview *stereo-matching* (Seitz *et al.* 2006)



The mesh becomes **textured** with the original photographs to form a 3D model

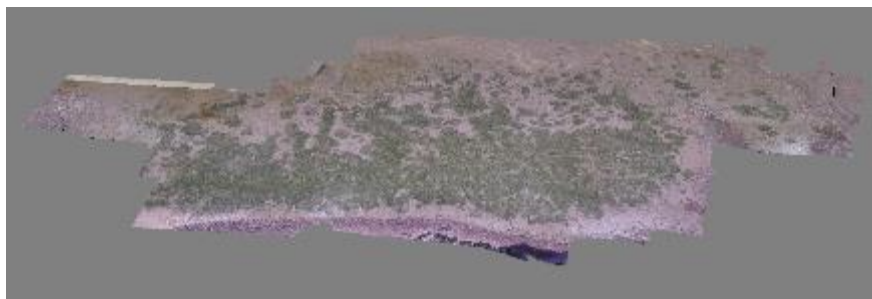


Figure 7 Steps used to create a three-dimensional model in Agisoft PhotoScan Professional (Details in italics represent the specific algorithms used and the layer present in the images is displayed by bold font). Source: L, Pratt, 2016, using PhotoScan 1.2.0.

Table 6 Parameters used in the steps to generate orthomosaics and DEM's from aerial data in Agisoft Photoscan Pro 1.2.0.

Align Image		Dense Cloud	
Accuracy	Medium	Quality	Medium
Pair pre-selection	Generic	Depth filtering	Aggressive
Key point limit	40,000		
Tie point limit	4,000		
Mesh		Texture	
Surface type	Height field	Mapping mode	Generic
Source data	Sparse cloud	Blending mode	Mosaic
Face count	Medium (30,000)	Texture size/count	4096 x 1
Interpolation	Enabled		
Point classes	All		

then imported as a raster image into ArcMap 10.2.2 where composite habitat maps were generated by combining the different spectral bands. This enabled *Z. noltii* boundaries to be analysed using image classification methods (Dugdale 2007; Meyer 2008; Jackson *et al.* 2011) (Appendix 2) and compared to the GIS polygon, created by GPS points recorded on foot. At study sites where a modified Xiaomi Yi Action Camera (NIR/Blue filtered) was used, the Normalised Difference Vegetation Index was calculated (Barille *et al.* 2009; Valle *et al.* 2015) by combining the reflectance of the red and infrared red colour bands (Tucker 1979), to assess the quantity of green biomass. However, it was often difficult to distinguish between *Z. noltii* and other vegetation including microphytobenthos and *Ulva spp* (Bunker 2008), therefore further ground truthing was required.

$$\text{NDVI} = \frac{\text{NIR} - \text{R}}{\text{NIR} + \text{R}}$$

$$\text{NIR} + \text{R}$$

NIR = Neo-infrared band

R = Red band

2.4 Morphological measurements

Random point sampling in meadows with relatively firm substrata was used in addition to the aerial images and walking the meadow boundary, to confirm the present of *Z. noltii* and check the accuracy of the UAV data. It also enabled the

health and condition of *Z. noltii* meadows to be studied and using ArcMap 10.2.2, 30 random waypoints were generated within the meadow boundary. This not only avoided bias but was more time efficient whilst in the field, as the points were loaded and easily located on the Garmin GPSmap 61/GPSmap 62stc. Each waypoint was sampled with a 50cm by 50cm stainless steel quadrat where the standard Seagrass-Watch parameters were recorded (McKenzie *et al.* 2003). This included *Z. noltii* presence/absence, seagrass percentage cover, shoot density, average canopy height, average canopy width, algae cover, epiphyte cover, substrate and any other seagrass species or organisms present. All surveyors were trained according to the same methodology in order to confirm consistency between results and multiple readings of some parameters such as percentage cover were taken to ensure quality assurance (Bunker 2008). Estimations of percentage cover recorded in the surveying were based on the area covered by the rooted plants and followed previous guidelines for the species (Mazik and Boyes 2009). When the percentage cover was estimated to be less than 5%, the number of individual shoots was recorded and the replicate data was then averaged in order to provide a representative mean percentage cover and shoot density for the entire meadow. At least 95% of the quadrats were also photographed to ensure standardisation, calibration of observers and to provide a permanent record to be used in further tools such as the citizen science app, 'SeagrassSpotter' (www.seagrassspotter.org).

2.5 Seed coring

Seed coring was carried out to monitor seagrass resilience at sites where *Z. noltii* was present and to assess the viability of the technique. At sites where *Z. noltii* was absent, 30 cores were also taken to indicate any signs of colonisation and potential future distributions. Furthermore, the process of coring (summarised in Figure 8) removed any bias from the winter die off.

2.6 Data Analysis

All morphological values were reported as means (\pm SD) unless stated otherwise. Prior to analysis all data was tested for normality using Shapiro-Wilk in R (R Core Team 2013) to meet the assumptions of parametric tests. However, if the data failed to conform to the normal distribution, alternatives to the parametric tests were used.



Figure 8 The process of coring; 1) Cores taken randomly (alongside random point sampling) with a standard PVC seed corer (50mm diameter x 250mm long) and cap (Mckenzie *et al.* 2003), pushed approximately 10cm deep into the substratum; 2) Sediment placed in stainless steel sieve (1-2mm mesh); 3) Sieved sediment using a little water and 4) Analysis of core content, where the number of whole seeds and half seeds retained was recorded. Seeds were then returned to the sediment to reduce core-induced disturbance. Image source: authors own, 2016.

Simple statistical tests such as two-sample t-tests and one-way ANOVA were conducted to identify any differences in the mean *Z. noltii* values obtained. Kruskal-Wallis was used as an alternative non-parametric form of ANOVA, to test the difference in habitat characteristics across study sites and Pearson product-moment correlation coefficients were carried out to assess correlations between variables such as rate of expansion/regression, seed density and *Zostera* Index Condition (ZCI). Both simple linear (SLR) and non-linear regression models were used to identify and predict associations between variables (current vs historical *Z. noltii* extent and NDVI vs seagrass morphometric results). Polynomial regression was referred in this study due to a higher degree of accuracy obtained from increased R^2 values.

Each morphometric variable recorded as part of this study measured different aspects of seagrass status. In order to identify which aspects presented most variability a principal component analysis (PCA) was conducted (Zar 1984; Johnson and Gage 1997; Salita *et al.* 2003). Principal components (PCs) with eigenvalues greater than 200 were considered, with variables less than or equal to -0.4 or greater than 0.4 being selected as dominant in each component. A general linear model (GLM) was then conducted using the dominant variables from the PCA and other environmental factors to determine the differences between the habitat

characteristics (**model:**, **family:**). Furthermore, a *Zostera* condition index (ZCI) was calculated using the dominant components, based on previous techniques used to measure habitat health (McKenzie *et al.* 2012, 2014; Wilde 2016). All of the habitat characteristics were perceived to represent a healthier meadow when higher (Krause-Jensen *et al.* 2004) and the ZCI score ranged from 0-1, with 1 being the healthiest meadow.

3.0 Results

3.1 *Z. noltii* extent

At 11 of the 21 study sites *Z. noltii* was found to be present, with seagrass meadows covering a total of 73.3 hectares along the South and West Wales coastline (Table 7). The Loughor estuary and Milford Haven Waterway harboured all the seagrass populations found, with significantly more *Z. noltii* being located in Pembrokeshire (83.4%) compared to Carmarthenshire (16.5%). Mapping using the transects technique was conducted at the two larger study sites (AB and PE), although did not deem as effective as using the handheld GPS (Figure 9). *Z. noltii* populations were found at the Burry Pill study site but due to the extremely sparse distribution and small meadow size (<1m²) seagrass morphometric sampling did not take place. No *Z. noltii* was found in Ferryside, Oxwich and Swansea Bay despite the historical presence (Kay 1998). There was also an absence of *Z. noltii* in Glamorgan, despite being predicted as a suitable habitat for *Z. noltii* to grow (Brown 2015).

The size of *Z. noltii* meadows ranged from small isolated patches only 0.159ha in size (LS1), to 40.7 ha of extensive seagrass (AB) (7.3±12.3). *Z. noltii* populations at Llanrhidian Sands and Sprinkle Pill displayed signs of regression (-16.2%yr⁻¹±6.0) although it was difficult to quantify any change due to the extremely small meadow size. No detectable change was observed at Garren Pill (-0.008%yr⁻¹). Signs of expansion were observed at the remaining study sites (16.6%yr⁻¹±15.2), displaying an overall average expansion of 2.0%yr⁻¹±20.7 (median = 1.8%yr⁻¹) for *Z. noltii* meadows in South and West Wales. Although, there was no significant difference between the mean historical *Z. noltii* area compared to the meadow area calculated from this study (t (9) = 0.2382, p = 0.817), a significant positive correlation was observed between the two variables (r = 0.786, t (15) = 4.917, p < 0.001). Using a non-linear regression model the current (2016) extent of *Z. noltii* meadows that were unable to be mapped in this study, was predicted (Figure 10).

Table 7 Surface area of *Z. noltii* at the 10 study sites where seagrass was found to be present along the South and West Wales coastline (The year displayed in italics indicates the actual year in which field sampling took place, if it differs from the citation). Historical data of the Pembroke River study site that could not be sampled in this study is stated, but not included in the overall Mean % rate of change, μ (yr^{-1}), observed.

Study Site	Size of <i>Z. noltii</i> Meadow (Ha)													Mean % rate of change, μ (yr^{-1})	
	(Hodges and Howe 2007) 1996	(Mazik and Boyes 2009) 2004	(Bunker, 2008)	(CCW GIS layer, 2008)	(Howson 2012) 2009	(Nikitik 2015) 2009	(Nikitik 2015) 2010	(Crook, Unpublished) 2011	(Nikitik 2015) 2011	(Nikitik 2015) 2012	(Natural Resources Wales GIS layer, 2013)	(Nikitik 2015) 2013	(Nikitik 2015) 2014		Current size from this study
Llanrhidian Sands 1 (LS1)	-	1.05	-	-	-	-	-	-	-	-	1.51	-	-	0.16	-18.43
Llanrhidian Sands 2 (LS2)	-	-	-	-	-	-	-	6.60	-	-	-	-	-	0.68	-17.94
Llanrhidian Sands 3 (LS3)	-	4.41	-	-	-	-	-	-	-	-	1.16	-	-	0.88	-7.41
Penclawydd (PE)	-	1.63	-	-	11	-	-	-	-	-	7.37	-	-	11.64	23.77
Angle (AB)	5.22	-	27.19	-	-	-	-	-	-	-	32.77 * recorded in Duggan - Edwards and Brazier, 2015.	-	-	40.68	16.07
<i>Pembroke River (PR)</i>	-	-	-	-	-	89.9	92.6	-	91.7	88.9	97.3	94.1	93.7	N/A	0.04
Pwllcrochan (PW)	-	-	-	-	-	-	-	-	-	-	1.79	-	-	3.85	38.34
Pembroke Dock (PD)	-	-	-	-	-	-	-	-	-	-	3.20	-	-	3.49	3.01
West Williamson (WW)	-	-	-	-	-	-	-	-	-	-	6.56	-	-	6.92	1.82
Garrens Pill (GP)	-	-	-	4.00	-	-	-	-	-	-	4.95	-	-	4.65	-0.01
Sprinkle Pill (SP)	-	-	-	-	-	-	-	-	-	-	0.87	-	-	0.32	-20.90
													Average	7.33±12.25	2.04±20.68

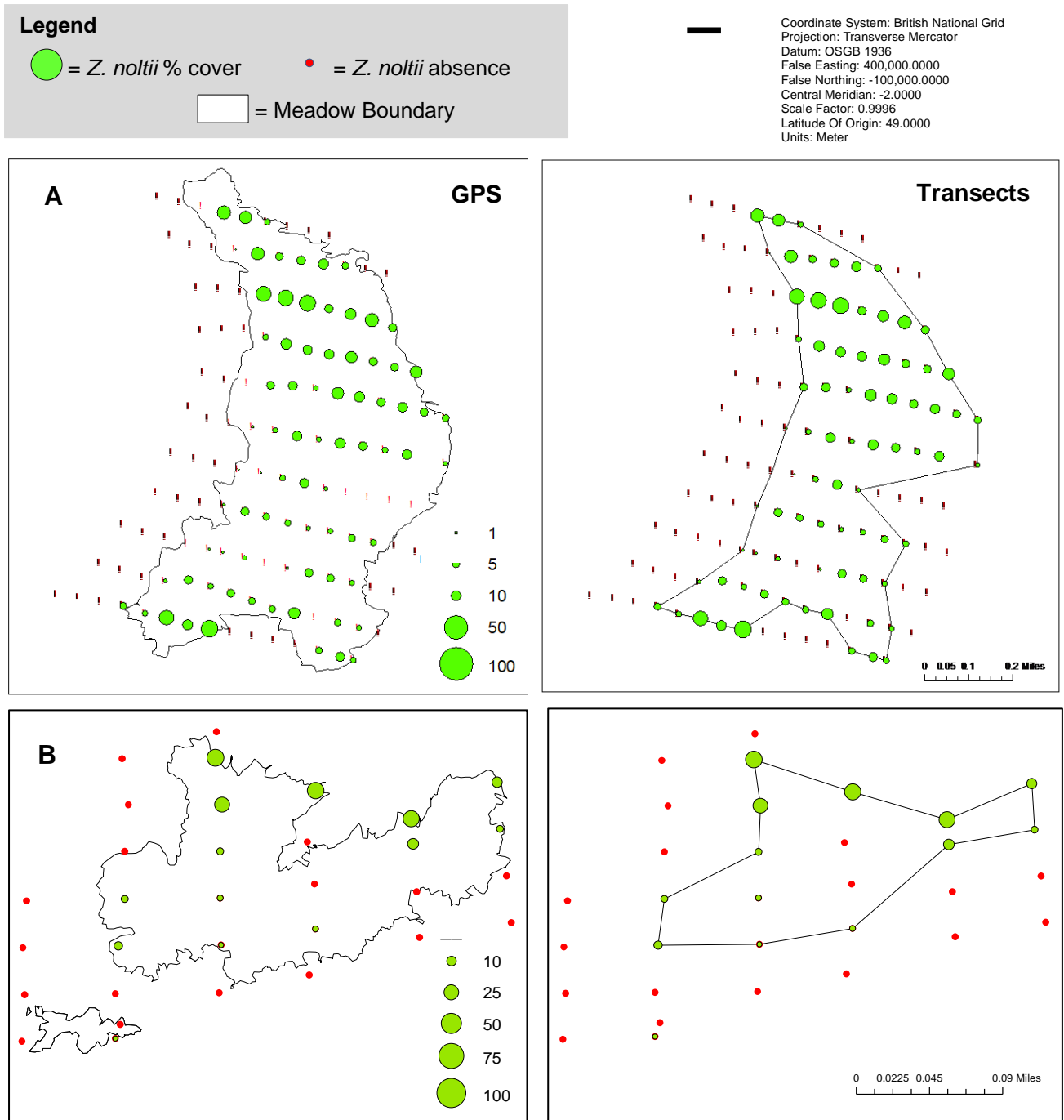


Figure 9 Differences in the area of seagrass recorded by 1) using a handheld GPS and 2) using transects, to assess different forms of methodologies in monitoring larger *Z. noltii* meadows (A, Angle Bay and B, Penclacwydd). Methods using the handheld GPS were more accurate with 34.6% more *Z. noltii* recorded at Angle and 205% at Penclacwydd, respectively. However, changes in the spatial distribution within a meadow could not be monitored therefore further monitoring should look at incorporating both methods, with transects on a smaller scale. Source: L. Pratt, ArcMap 10.2.2, 2016.

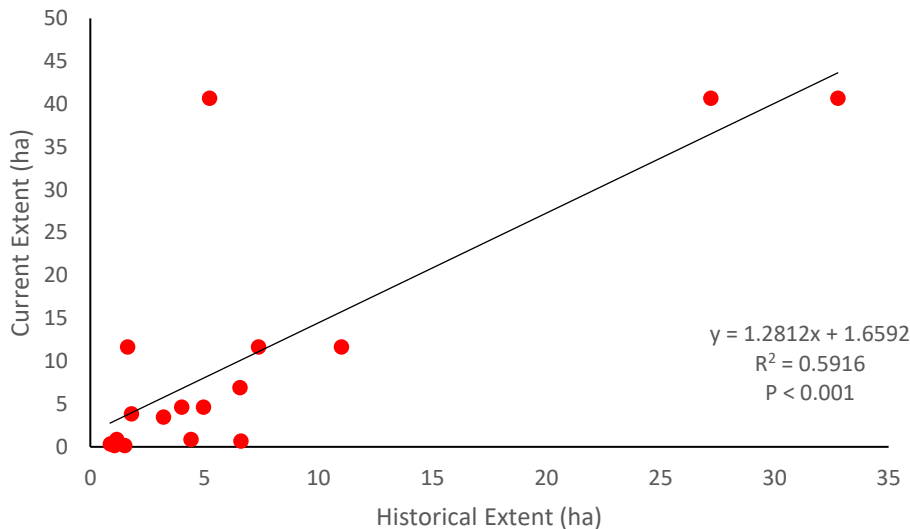


Figure 10 Simple linear regression (SLR) model that can be used to predict the current *Z. noltii* extent based on historical (<2016) distributions. Pembroke River *Z. noltii* populations are predicted to have a current area of 121.71 ha based on the model, although regression model is not site specific. *Add 95% CI to linear regression*

The spatial distribution of existing *Z. noltii* meadows along the South and West Wales coastline is also changing (Figure 11 and 12), with the expansion of the seagrass meadows taking place mainly in the lower intertidal zone. The upper shore meadow boundaries were limited by the increased elevation levels (max 12m above chart datum) and populations were also observed to be expanding further inland, towards the Salt Marsh (PE). At Pwllcrochan, *Z. noltii* populations were also observed to be colonising further sheltered areas along the coastline.

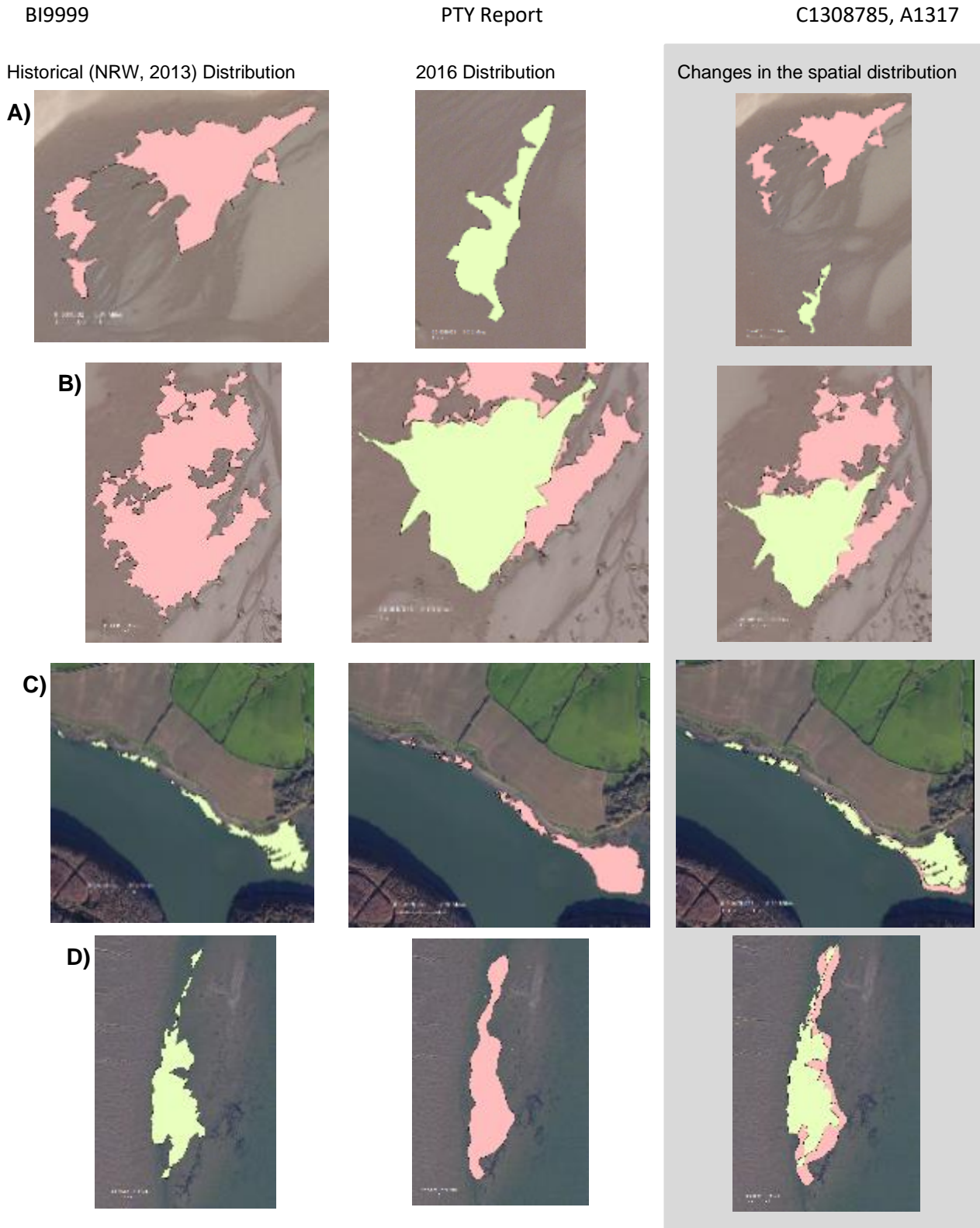


Figure 11 Evolution of the spatial distribution of *Z. noltii* from 2013 to 2016, at sites showing signs of localised regression; A) Llanrhidian Sands site 1 (LS1), B) Llanrhidian Sands site 2 (LS2), C) Garren Pill (GP) and D) Sprinkle Pill (SP). Llanrhidian 2 was not included in the figure, as no historical records of the sites spatial distribution were available. Areas in green represent to most recent NRW *Zostera* GIS layer (2013) and meadow boundaries displayed in pink are those generated from this study. *Z. noltii* was mapped using on foot a handheld GPS apart from GP, where a customized 3DR solo was used to map regions of *Z. noltii* on infirm substrata. Source: L. Pratt, ArcMap 10.2.2, 2016.

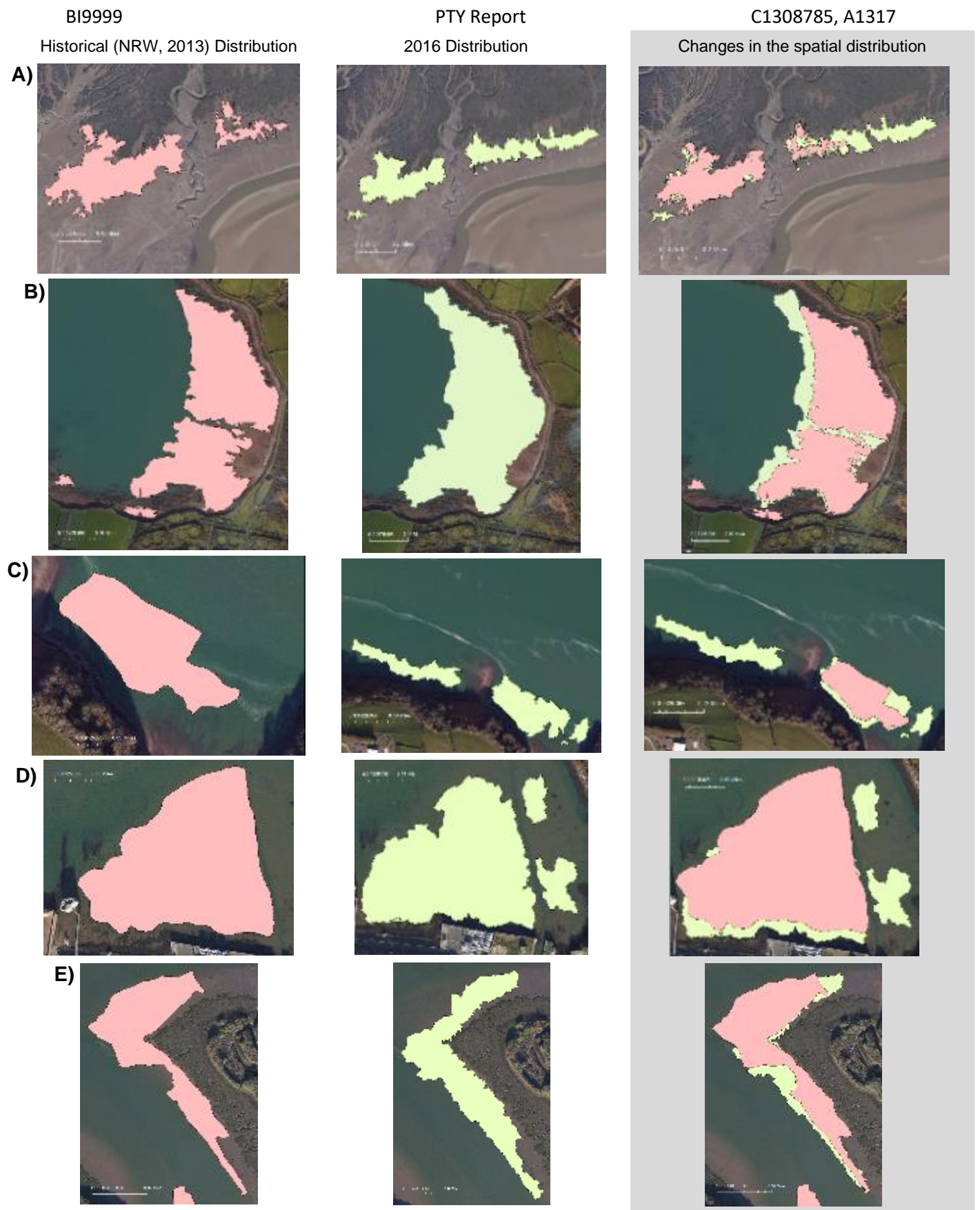


Figure 12 Evolution of the spatial distribution of *Z. noltii* from 2013 to 2016, at sites showing signs of localised expansion; A) Penclacwydd (PE), B) Angle Bay (AB), C) Pwllcrochan (PW), D) Pembroke Dock (PD) and E) West Williamson (WW). Areas in green represent to most recent NRW *Zostera* GIS layer (2013) and meadow boundaries displayed in pink are those generated from this study. *Z. noltii* was mapped using on foot a handheld GPS. Source: L. Pratt, ArcMap 10.2.2, 2016.

3.2 Drone analysis

Drone data was available for 2 of the study sites; Garren Pill where the substrata was too deep to access via foot and Pwllcrochan, where aerial imagery could be assessed against a known meadow boundary. Finer scale aerial data was also collected at Angle Bay and Garren Pill, to compare the use of UAV photographic mapping at relatively low and high seagrass densities. The use of a UAV at meadows differing in size and ability of each camera to map *Z. noltii* was also assessed. Aerial data capture permissions were obtained for all 3 of these sites, however could not be obtained for other locations including Pembroke River and West Williamson. A high number of recreational boat users also limited drone work at West Williamson and data image capture was prevented in the Burry Inlet due to high wind exposures.

The DJI Phantom 3 Professional was the simplest out of the 3 models to operate however, it is not designed for environmental mapping and the lack of waypointed flights meant mapping larger areas of dense *Z. noltii* (at sites such as AB) was extremely difficult. The ability to fly waypointed missions enabled by pixhawk driven 3DR drones made this form of remote sensing more effective and enabled extended areas of *Z. noltii* that were unable to be assessed by foot, to be mapped. The quality of each of the cameras and the ability to measure *Z. noltii* morphometric data differed with each model. At low altitudes the RICOH GR II RGB camera produced the brightest and texture with the clearest exposure, however the pixels often became distorted at high focus levels (Figure 13). The large area coverage and repeatability of the drone models used also displayed how this form of remote-sensing can be time efficient to smaller teams often working against strong tidal cycles (Table 8).

Table 8 Differences in the time spent using a handheld GPS and light weight UAV to map the spatial and temporal distribution of *Z. noltii* meadows.

Fieldwork Activity	Time taken on Handheld GPS (minutes)	Fieldwork Activity	Time taken on UAV (minutes)
Setting up GPS	5	Planning mission	15
Walking around meadow boundary	<i>*Dependant on size</i> 60 (small, e.g. PW) 120 (large e.g. AB)	UAV image acquisition flight	<i>*Dependant on model</i> ~20
Collection of seagrass morphometric samples	120	Collection of seagrass morphometric samples	120
Total	3 hours 35 minutes		2 hours 35 minutes

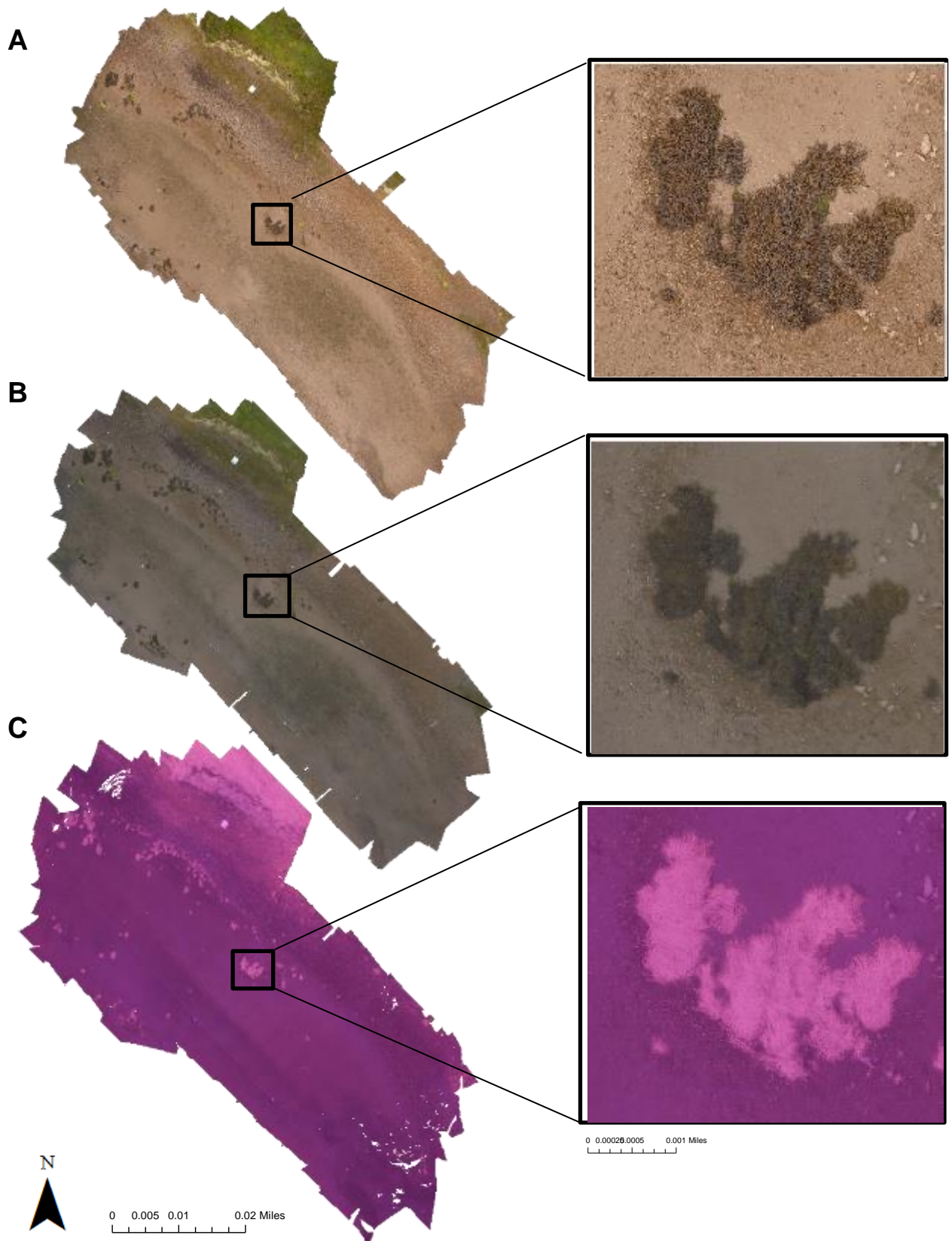


Figure 13 Differences in the quality of the aerial data recorded at Garren Pill, July 2016, on a customized 3DR Solo, flown at 15m using; A) RICOH GR II consumer grade compact camera, B) modified Xiaomi Yi Action Camera (RGB) and C) modified Xiaomi Yi Action Camera (NIR/Blue filtered). Ground resolution altered with each camera from 3.96 mm/pix on the RICOH, 4.57mm/pix on the RGB Agrocams and 4.53 mm/pix on the NIR/Blue filtered Agrocams.

RGB Aerial data captured from the drones, indicated that meadow boundaries generated from the handheld GPS often provided an overestimate to the extent of *Z. noltii* present at each study site (Figure 14), not taking into account differences in spatial distribution across a meadow. Visual interpretations of unsupervised (Figure 15) and supervised classifications also identified a similar problem, with large areas of microphytobenthos and nearby marshland often being misclassified for *Z. noltii*. Supervised classifications displayed higher levels of accuracy than unsupervised analysis (Figure 16), with the density of *Z. noltii* also influencing the affectability of the classification. Whilst dense areas of *Z. noltii* were frequently detected and easily mapped, sparse populations (<20% coverage) were often not identified. This highlighted the difficulty in using spectral classifications from 3-band imagery to determine seagrass cover and manual classification of the *Z. noltii* meadows was then implemented to achieve accurate meadow boundaries of the study sites (Figure 17). The NDVI results also supported this as little visible difference was observed between *Z. noltii* populations and surrounding vegetation (Figure 18). However, the calculated NDVI values did allow *Z. noltii* areas to be differentiated from other intertidal habitats, displaying an index >0.3 (Figure 17).

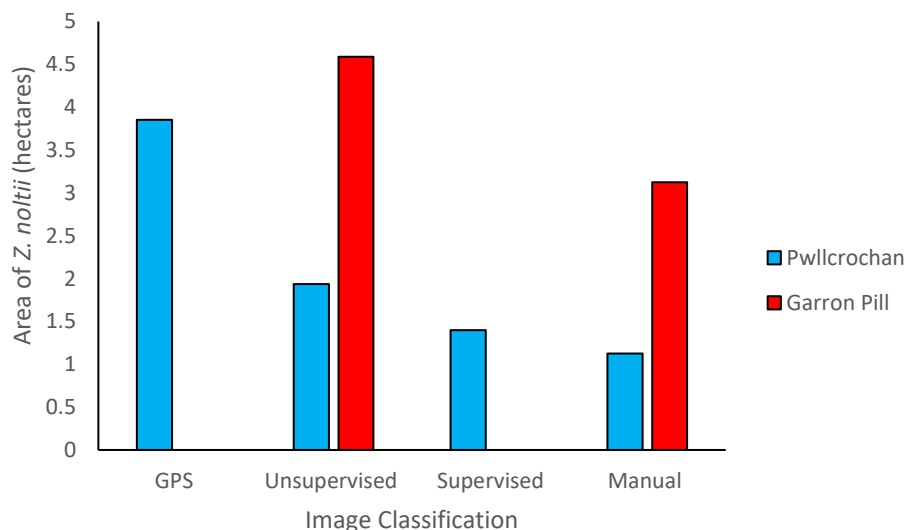


Figure 14 Differences in the area of *Z. noltii* at A) Pwllcrochan and B) Garron Pill, recorded using Garmin GPSmap 62 and forms of classification of the UAV data carried out on ArcMap 10.2.2.

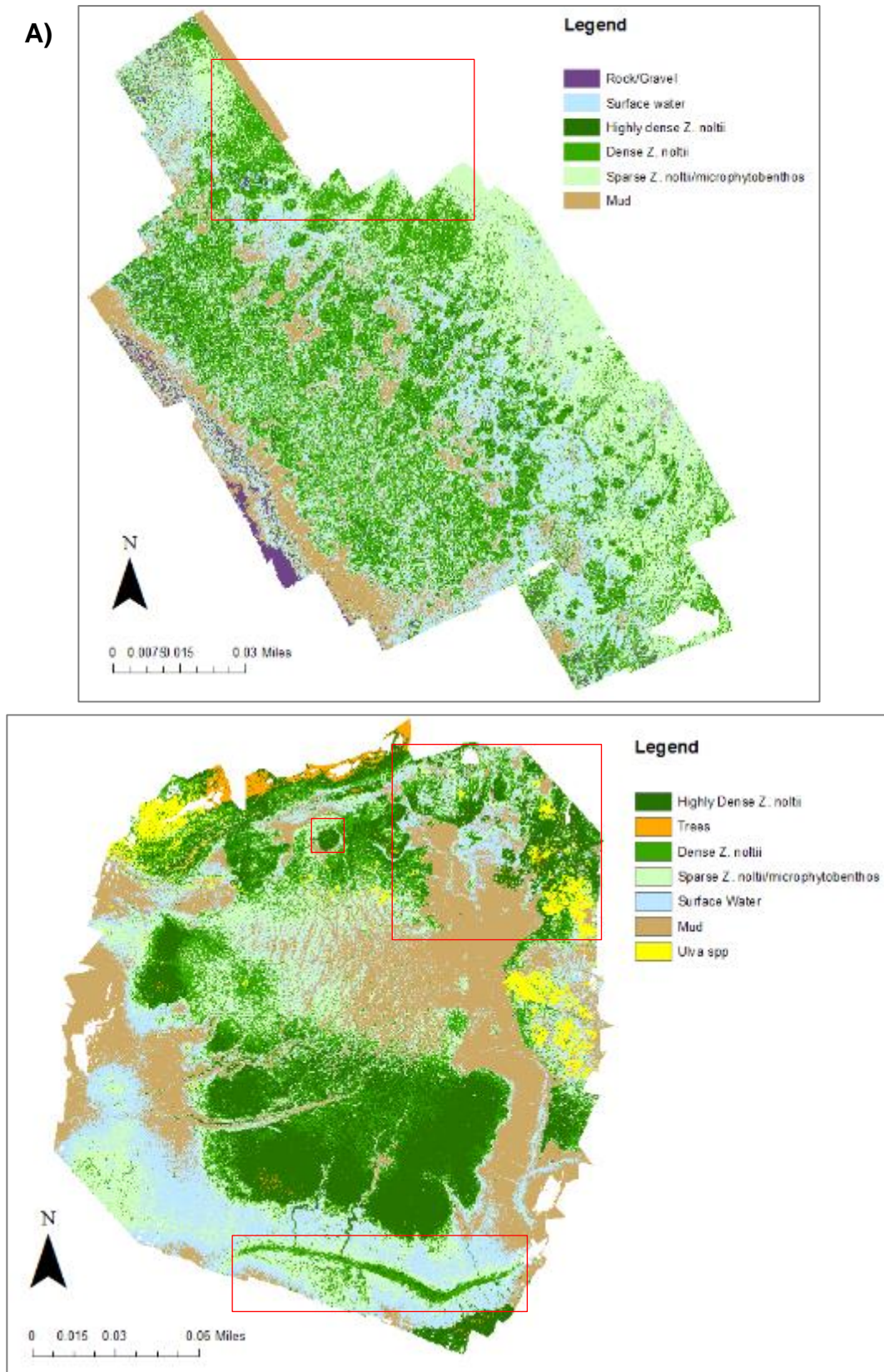
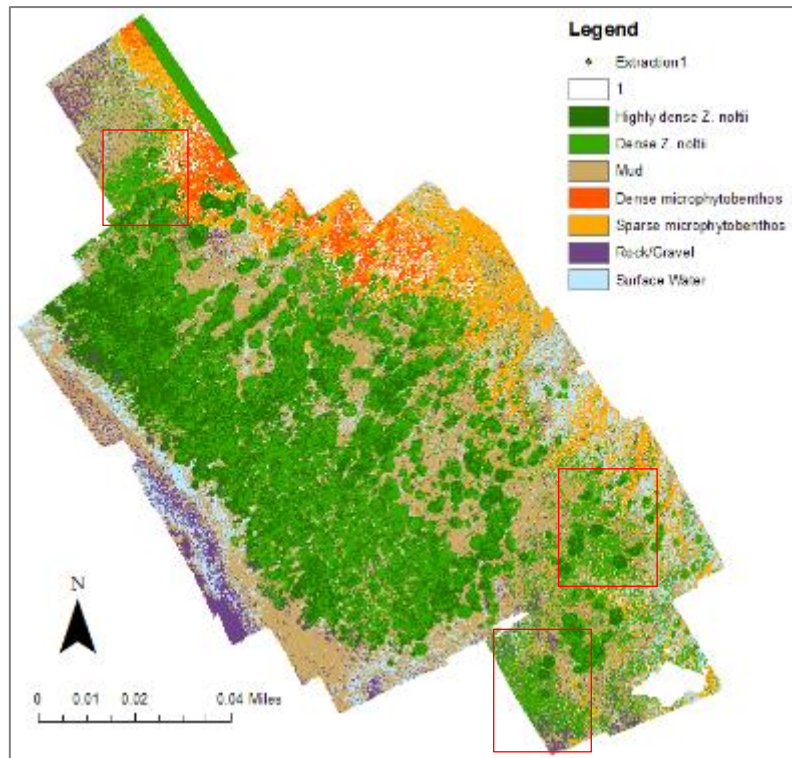


Figure 15 Unsupervised ISO Cluster classification of true-colour mosaics at both A) Pwllcrochan (30m) and B) Garren Pill (50m). Average accuracy of the classifications was 53.3% (K = 0.33 observed at Pwllcrochan, K = 0.42 observed at Garron pill) (Appendix 3). Red boxes indicate areas that display the same pixel type as *Z. noltii*, providing an over estimate of meadow area. Source: L. Pratt, ArcMap 10.2.2, 2016.



****Complete Garren Pill Supervised Classification**

Figure 16 Supervised Maximum Likelihood image classification (MLC) of true-colour mosaics at both A) Pwllcrochan and B) Garren Pill. Average accuracy of the classification was(K=0.48 at Pwllcrochan and K = ... observed at Garron Pill) (Appendix 4). Red boxes indicate areas that display the same pixel type as *Z. noltii*, providing an over estimate of meadow area. Source: L. Pratt, ArcMap 10.2.2, 2016.

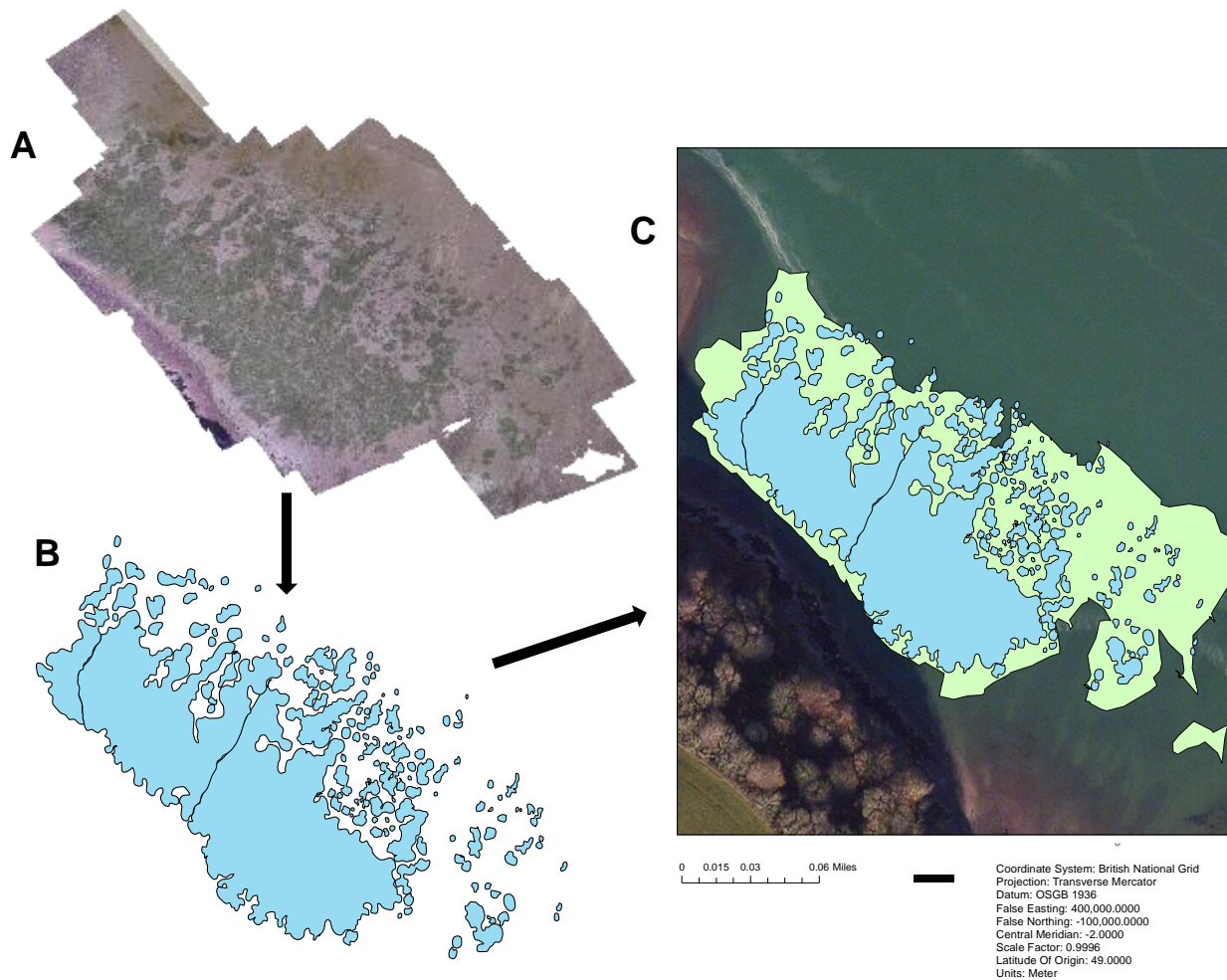


Figure 17 The process of manual classification used to assess *Z. noltii* boundaries at Pwllcrochan; (A) The texture generated from PhotoScan Professional Version 1.2.0, (B) The meadow boundary generated from drawing polygons round the dense *Z. noltii* observed in the aerial imagery using ArcMap 10.2, displaying a more clumped seagrass distribution and (C) Comparison between the size of the meadow boundary recorded from the DJI Phantom 3 Professional (1.2 ha, displayed in blue) to the data recorded on the portable GPS unit (3.9ha, displayed in green) (69.2% reduction). Source: Source: L. Pratt, ArcMap 10.2.2, 2016.

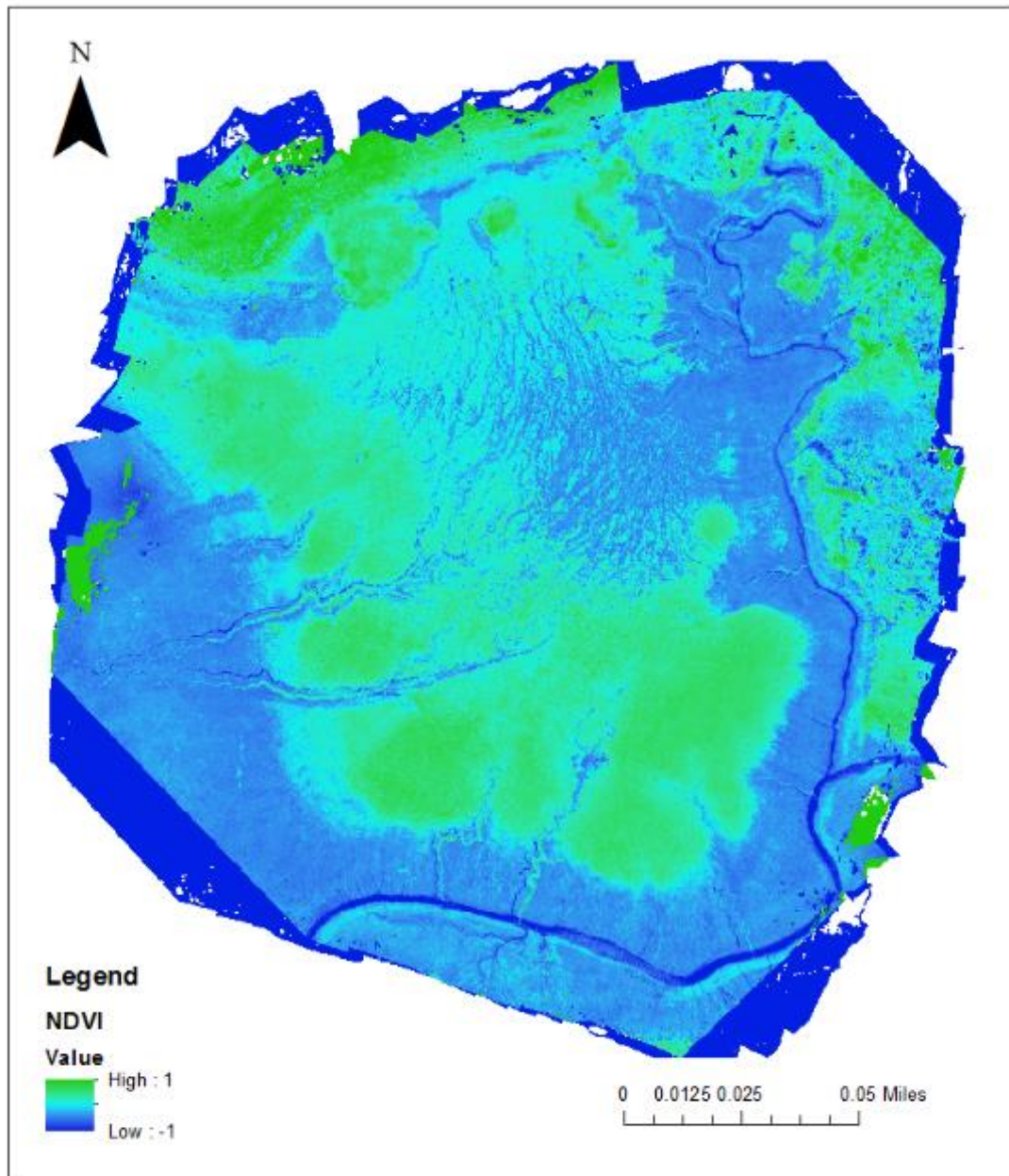


Figure 18 Relative NDVI map generated from true-colour and NIR imagery at taken using a modified Xiaomi Yi Action Camera, at Garron Pill, July 2016. Source: L, Pratt, ArcMap 10.2.2, 2016.

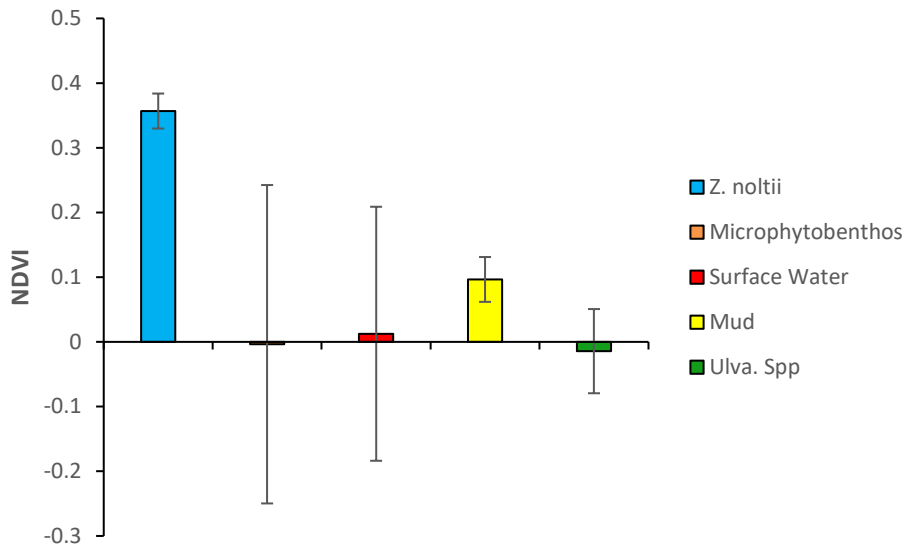


Figure 19 Differences in the NDVI (Means \pm 95% CI) calculated for the different spectral classifications of the intertidal aerial data (Appendix 3). The *Z. noltii* NDVI was significantly higher ($F(4) = 5.152, p < 0.001$) than that observed in the other classifications, meaning that seagrass species can be clearly identified through this form of image analysis.

3.3 Seagrass morphometrics

There was a distinct difference between the habitat characteristics of the 10 *Z. noltii* meadows studied (Figure 20). Shoot density ranged from 4.1 to 125.1 per 0.10m² (62.3±61.3), and varied significantly across the sites (H (9) = 157.2711, p < 0.001), with the highest values recorded at West Williamson and Pembroke Dock and lowest on Llanrhidian Sands in the Burry Inlet (Table 9). Seagrass canopy height was also significant across the different sites (H (9) = 81.128, p < 0.001), ranging from 43.4mm to 74.4mm (59.9±29.5), with the highest lengths found similarly at Pembroke Dock and lowest at Llanrhidian Sands. Seagrass percentage coverage ranged from 3.8% to 71.9% (33.3±31.4), with again the highest values distributed amongst the Pembrokeshire study sites and the lowest values observed at Llanrhidian Sands. There was a significant difference in the percentage cover recorded across the sites (H (9) = 178.8939, p < 0.001) and the estimation of these specific seagrass parameters by different surveyors, had no influence on the data collected (H (2) = 2.3678, p-value = 0.306). All 3 of the habitat characteristics mentioned above displayed a further significant difference between the average shoot density (t (297) = 11.9292, p < 0.001), canopy height (t (298) = 2.6946, p < 0.05) and percentage cover (t (298) = 13.0569, p < 0.001) observed at expanding *Z. noltii* meadows and beds displaying signs of regression. Expanding meadows therefore displayed a higher shoot density, percentage cover and canopy height. No correlation was observed between the in morphometric values and spatial heterogeneity at each study site (Appendix 3).

The sediment composition altered across sites, comprising of mud, mud/sand, sandy mud and mud/rock. The dense mud substratum was the most common, accounting for 37% of the 300 quadrats sampled. The sandy/mud sediment and the mud/sand substrate were also common representing 30% and 20% respectively, with mud/rock accounting for the remainder. Furthermore, the majority of study sites (82%) were identified as pure *Z. noltii* meadows, however, reduced *Z. marina* populations were found to inhabit the depressions and channels at specific study sites (PE and PW).

Table 9 Seagrass parameters recorded at 13 of the locations where *Z. noltii* was found to be present along the South and West Wales coastline.

Site	<i>Z. noltii</i> cover (%)	Shoot density (per/0.2m ²)	Leaf Length (mm)	Leaf width (mm)	Epiphyte cover (%)	Algae cover (%)
Llanrhidian Sands (Bed 1)	6.1±6.1	15.7±17.7	43.4±35.5	1.12±0.90	0.01±0.01	0.90±1.85
Llanrhidian Sands (Bed 2)	6.5±5.6	15.9±14.8	59.8±46.7	1.10±0.88	0.00±0.01	0.37±0.89
Llanrhidian Sands (Bed 3)	4.1±3.0	6.0±7.9	67.1±40.7	1.40±0.81	0.00±0.00	0.40±1.13
Penclawydd	21.5±15.6	46.4±24.7	47.7±11.8	0.95±0.30	0.00±0.00	0.00±0.00
Angle	30.5±24.5	64.0±41.4	46.4±17.5	0.94±0.37	0.01±0.04	0.10±0.40
Pwllcrochan	57.815±30.7	116.5±76.6	67.1±24.6	1.15±0.58	0.00±0.00	1.20±2.47
Pembroke Dock (West Llanion Pill)	66.1±30.0	116.8±66.6	74.4±16.8	1.56±0.52	0.00±0.00	0.53±2.22
West Williamson	71.9±23.0	125.1±61.7	79.4±22.9	1.43±0.51	0.00±0.00	4.03±7.32
Garrens Pill	44.8± 23.5	75.5± 31.0	66.7±14.3	1.23±0.44	0.01±0.01	0±0
Sprinkle Pill	24.3±18.8	41.2±43.9	47.1±14.6	1.03±0.18	0.0±0.00	0±0
Average	33.3±31.4	62.3±61.2	59.9±29.5	1.19±0.62	0.00±0.01	0.75±2.86

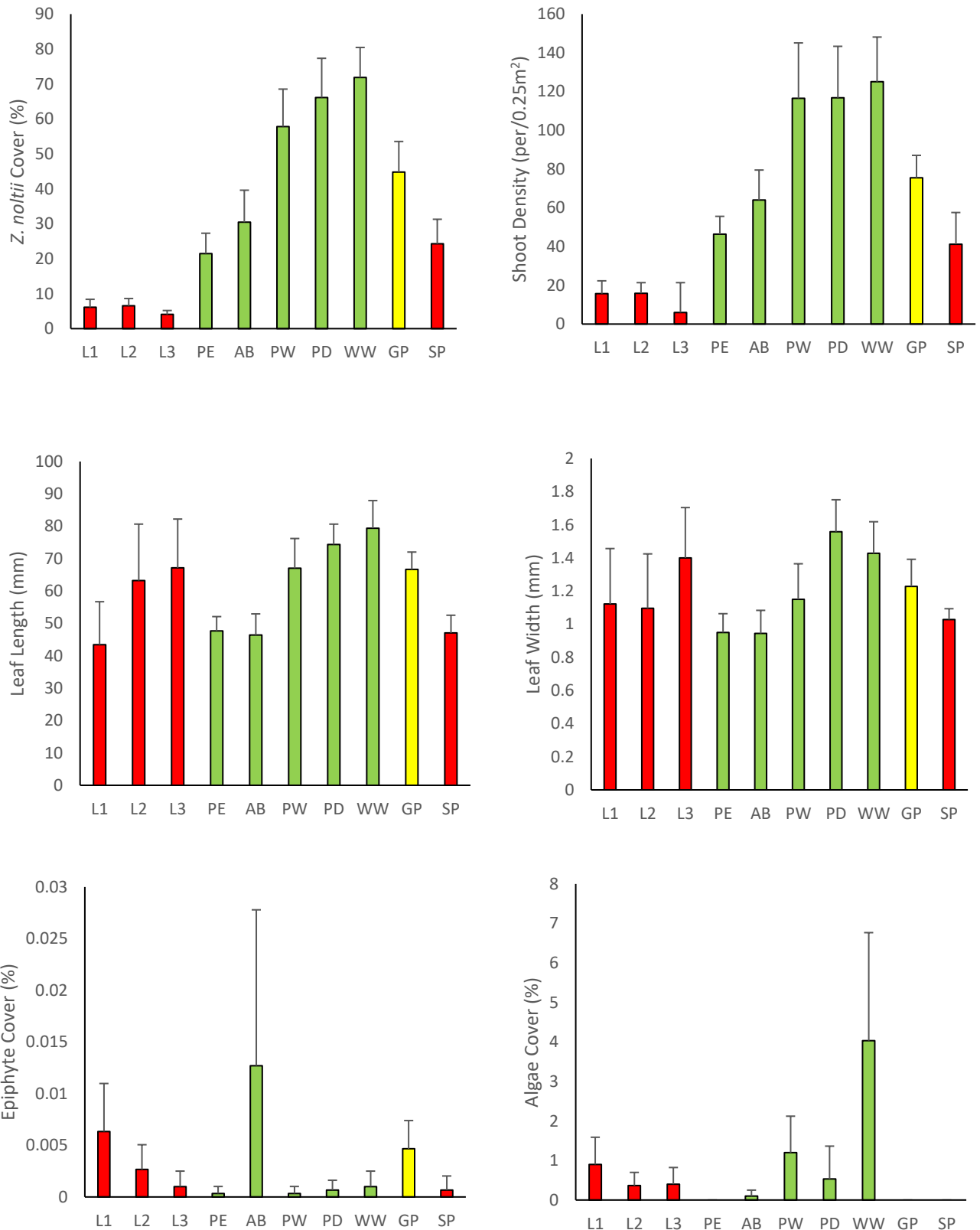


Figure 20 Mean ($\pm 95\%$ CI) *Z. noltii* cover, shoot density, leaf length, leaf width, epiphyte cover and algae cover across all 10 study sites. Green indicates values that were recorded in a *Z. noltii* meadow that displayed signs of expansion, yellow no detectable change in the meadow size and red, a *Z. noltii* meadow with observed regression correlations in the area.

3.4 Historical change in *Z. noltii* morphometrics

For 2 out of the 10 study sites historical changes over time of selected habitat characteristics can be studied. There was a significant difference in the mean *Z. noltii* cover ($F(7) = 5.727$, $p < 0.05$) and canopy height ($F(5) = 8.111$, $p < 0.05$) recorded from 1996 to 2013 at Angle Bay (Figure 21). However, no clear correlation was observed in either of the seagrass morphometric values despite the increasing aerial extent of the study site, mostly likely due to differences in methodologies. Seasonality may also have influenced any correlations as differences in the coverage of *Z. noltii* between April and June 2016 displayed how there was a significant increase in the *Z. noltii* cover within these 3 months ($t(58) = -4.3269$, $p < 0.05$) to give a mean of 53.8 ± 16.5 .

Coverage data taken from the second Llanrhidian Sands site also displays an increase in seagrass cover from 5.7 ± 6.8 in 2011 to 6.5 ± 5.6 in 2016, although there was no significant difference between the means ($t(129) = -0.5825$, $p = 0.5612$) and seasonality is likely to have had a similar effect on the results. However, there was a significant increase in the shoot density per/0.25m² at Llanrhidian 2 ($t(129) = -2.945$, $p < 0.05$) despite the decrease in *Z. noltii* extent. The lack of extensive *Z. noltii* surveying and accessible data meant that any further data analysis with historical seagrass morphometrics was heavily limited.

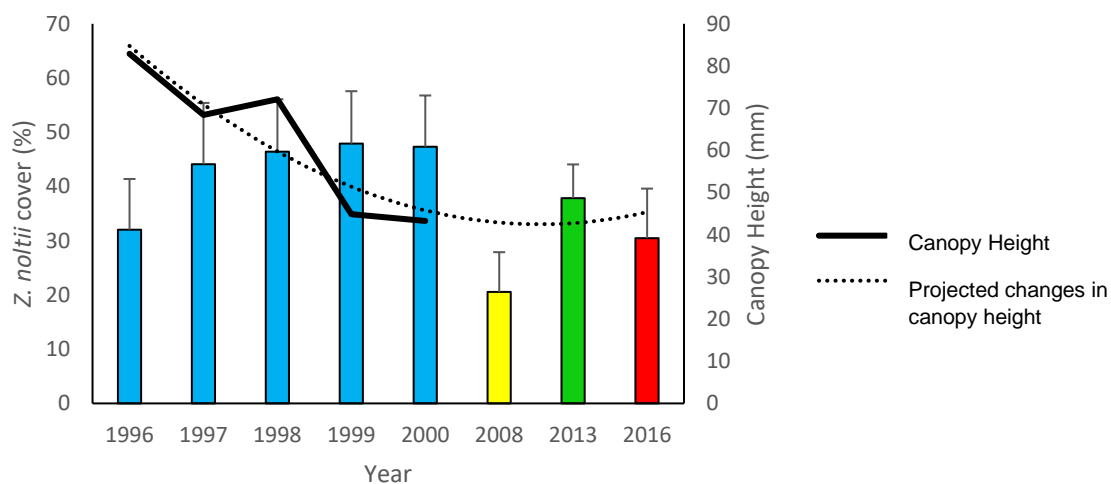


Figure 21 Changes in the average *Z. noltii* cover (Means \pm 95CI) and mean canopy height (mm) observed at Angle Bay from 1996 to 2000. Blue indicates historical values obtained from Hodges and Howe, 2007, yellow, Bunker, 2008, and green, Duggan-Edwards and Brazier, 2015, with the shoot density values obtained from the same data source.

3.5 Multivariate analysis of morphometric variables

From my morphometric measurements, in order to determine which characteristics contributed most to the variability within and between the different study sites, a principle component analysis (PCA) was conducted. Two PCAs had eigenvalues greater than 200 and together accounted for 96.5% of the variation (Table 10). The first principal component (PC1) was the most important, having an eigenvalue of 4720 and contributing to 84.2% of the variance. The component was dominated by average *Z. noltii* percentage cover and shoot density, with the axis suggested to be loosely representative of abundance, where an increase in PC1 represents an overall increase in the *Z. noltii* density (Figure 22). The second principal component (PC2) had a smaller eigenvalue of 692 and contributed to 12.3% of the variation amongst the data, with the only variably dominant variable for PC2 was average canopy height.

Table 10 PCA results of 10 *Z. noltii* sites sampled along the South and West Wales coastline (Coefficients in bold represent the dominant variable in each principal component). For principal component scores see Appendix 6.

	Principal Component 1 (PC1)	Principal Component 2 (PC2)
Summary Values		
Eigenvalues	4720	692
% Variation	84.2	12.3
Cumulative % Variation	84.2	96.5
Seagrass Morphometrics		
Average <i>Z. noltii</i> percentage cover	0.418*	-0.020
Shoot Density	0.883*	0.245
Average Canopy Height (mm)	0.214	-0.969*
Average Canopy Width (mm)	0.003	-0.015
Epiphyte percentage cover	0.000	0.000
Algae percentage cover	0.005	-0.018

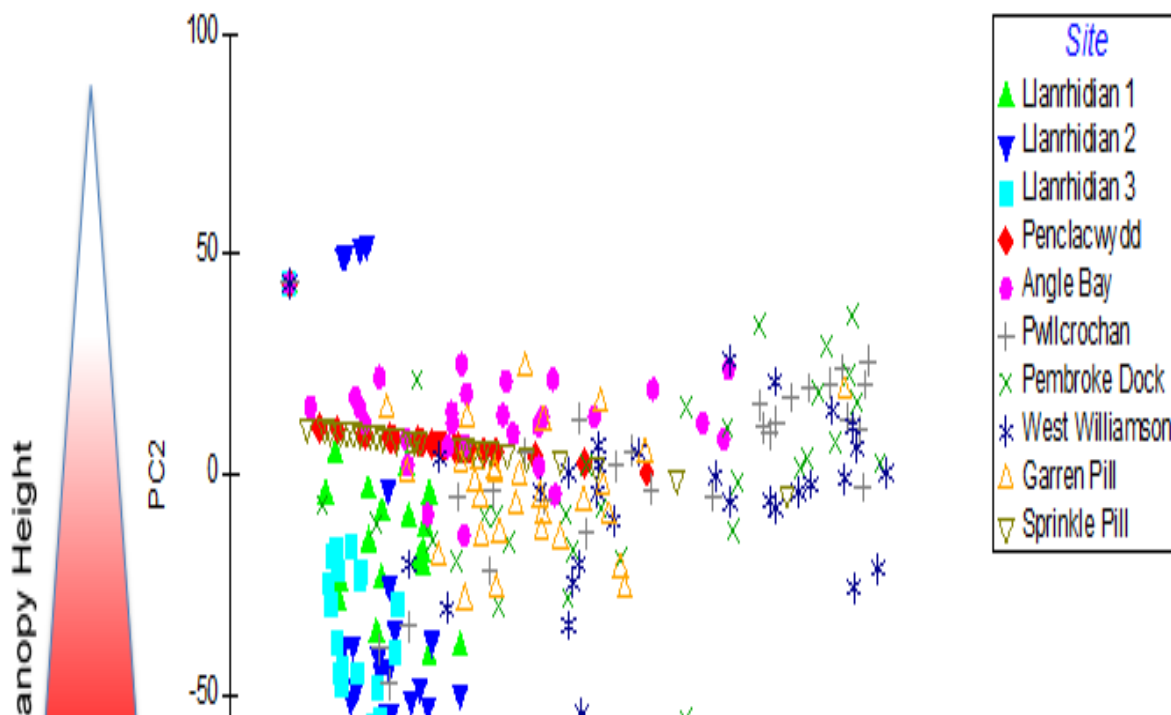


Figure 22 Principal component analysis (PCA) of seagrass characteristics from 10 different study sites, spread along the South and South West Wales coastline.

From the results of my principal analysis component, a general linear model (GLM) was conducted to study the difference between the dominant components at each of the sites. The influence of various factors including seasonality, sediment type, and elevation were also accounted for. As expected *Z. noltii* cover had a significant influence over the shoot density ($p < 0.001$) and canopy height ($p < 0.001$) recorded (Appendix 6). Shoot density however, has no influence over the canopy height observed ($p = 0.298$). The sediment type had a significant influence on *Z. noltii* cover ($p < 0.05$, $p < 0.05$, $p < 0.001$, respectively) whilst elevation ($p = 0.915$, $p = 0.523$, $p = 0.542$; GLM) and seasonality ($p = 0.989$, $p = 0.611$, $p = 0.527$; GLM) did not significantly influence the data.

3.6 *Zostera* Condition Index

The 3 dominant components from the PCA, were used to indicate habitat health and *Zostera* condition. Each study site was scored and ranked (Table 11) on their respective condition, with the ranking suggesting that West Williamson is the

healthiest *Z. noltii* meadow sampled with a score of 11. Study sites at Llanrhidian Sands had the poorest result with a seagrass health scores no greater than 6,

Table 11 Report card for the seagrass condition for *Z. noltii* meadows in the South and West Wales region (March – July 2016). *Zostera* condition score and index (ZCI) were calculated using seagrass cover, shoot density and canopy height. Dark green indicates very good condition, green is good condition, yellow is moderate condition, orange medium poor condition and red very poor condition.

Site	<i>Z. noltii</i> cover (%)	Shoot Density (per/0.2m ²)	Canopy Height (mm)	<i>Zostera</i> Condition Score (ZCS)	<i>Zostera</i> Condition Index (ZCI)
L1	1	1	3	5	0.33
L2	1	1	3	5	0.33
L3	1	1	4	6	0.33
PE	2	2	3	7	0.47
AB	2	2	3	7	0.47
PW	3	3	4	10	0.67
PD	3	3	4	10	0.67
WW	3	4	4	11	0.73
GP	2	2	4	10	0.67
SP	2	2	3	7	0.47

<i>Z. noltii</i> cover (%)	Rank
>80	5
60 - <80	4
40 - <60	3
20 - <40	2
>20	1

Shoot Density (per/0.2m ²)	Rank
>160	5
120 - <160	4
80 - <120	3
40 - <80	2
<40	1

matching the results of the multivariate analysis. A Pearson product-moment correlation coefficient was then used to assess the relationship between ZCI and change in the area extent of the *Z. noltii* meadows. A positive correlation was displayed between the mean % rate of change (yr^{-1}) (Appendix 3) and ZCI although was not significant ($r = 0.2390563$, $df = 8$, $p\text{-value} = 0.506$).

3.7 *Z. noltii* morphometrics vs NDVI

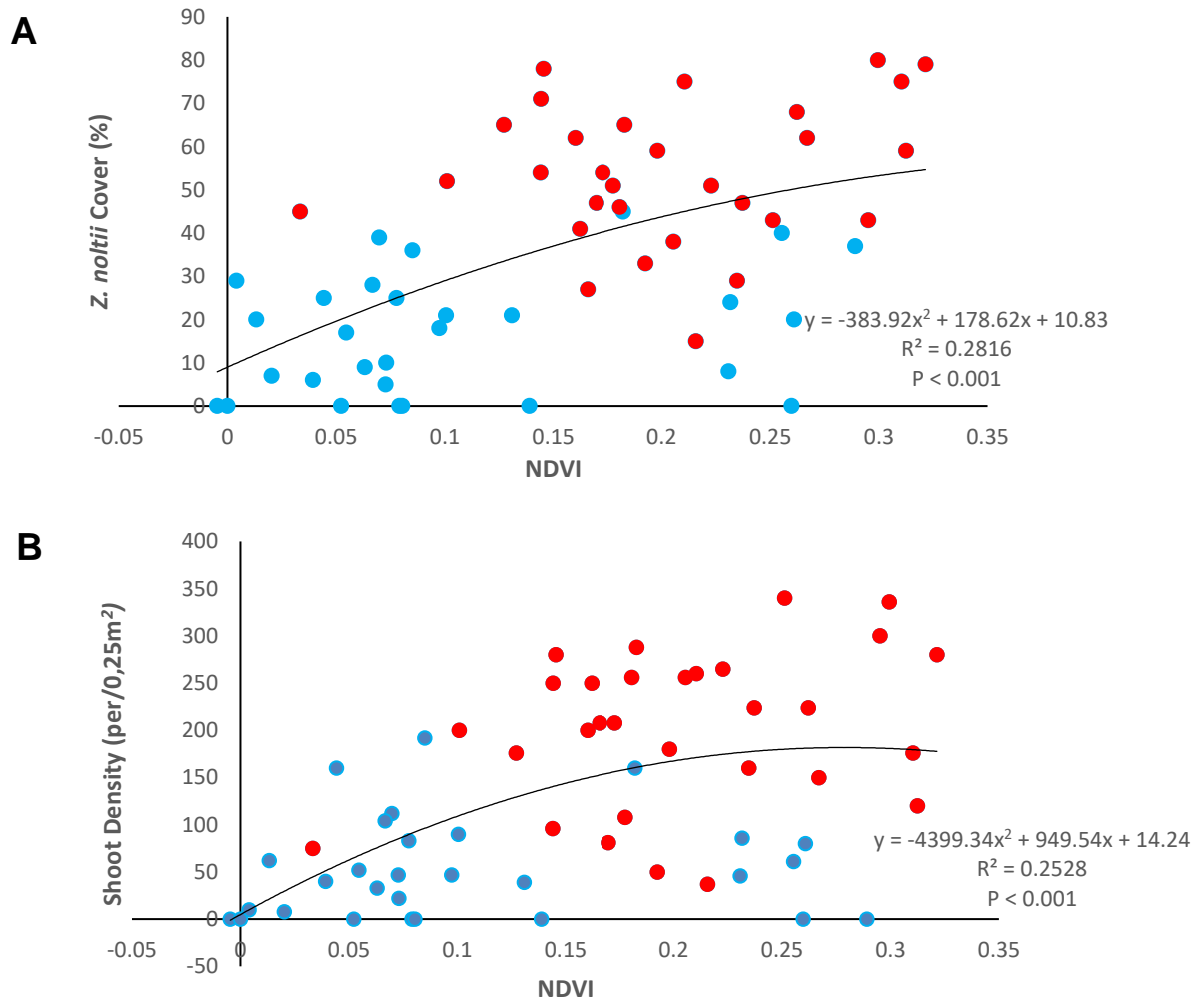
There was a positive relationship between NDVI and dominant *Z. noltii* habitat characteristics (Figure 23), proving consistent with previous analysis (Valle et al. 2015). Significance in the correlation was observed between NDVI and Cover ($r = 0.471$, $df = 57$, $p < 0.001$) and NDVI and shoot density ($r = 0.383$, $df = 57$, $p < 0.05$) through Pearson Product Moment coefficients, indicating the potential of NDVI to monitor habitat health. However, the relationship between canopy height and NDVI displayed no significance ($r = 0.222$, $df = 57$, $p = 0.0912$) indicating the limitations of aerial data to monitor habitat health characteristics on a finer scale.

Canopy Height (mm)	Rank
>80	5
60 - <80	4
40 - <60	3
20 - <40	2
<20	1

3.8 Core Analysis

Seeds (half and full) were found at 9 of the study sites, with the total number of whole seeds found per site ranging from 0 to 3 (0.8 ± 1.2) (Figure 24). The average seed density per m^2 for the *Z. noltii* meadows along the South and West Wales coastline was 1.4 ± 2.1 and there were significantly more seeds obtained at sites where *Z. noltii* was known to be present ($t(20) = 3.2042$, $p < 0.05$). A Pearson product-moment correlation coefficient also indicated there was a significant positive correlation between average seed density per m^2 and ZCI ($r = 0.773$, $df = 20$, $p < 0.05$) (Appendix 4), and seed density and mean % rate of change, μ (yr^{-1}) ($r = 0.705$, $df = 20$, $p < 0.001$) (Appendix 5). Despite previous studies (Harrison 1993) no

significant correlation was observed between seed density and elevation of the *Z. noltii* meadow (Appendix 8), most likely due to the limited number of seeds recorded.



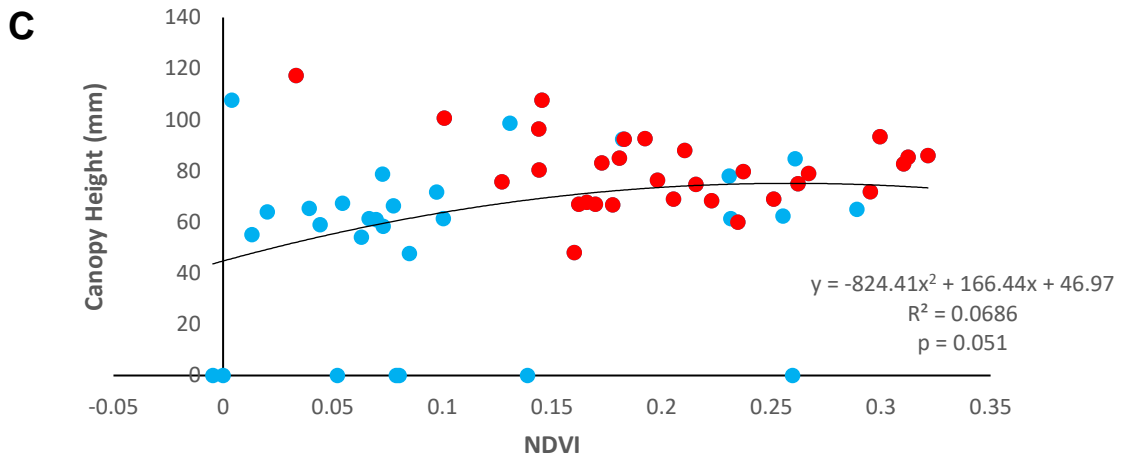


Figure 23 Non-linear regression model estimating the relationship between the

Normali:
 caracte
 height. F
 and blue
 calculat

at
 canopy
 in Pill

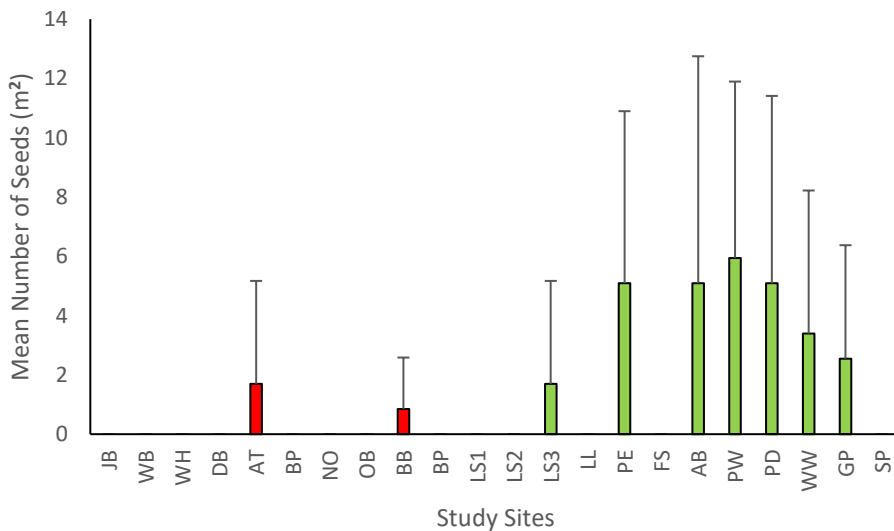


Figure 24 Mean ($\pm 95\%CI$) *Z. noltii* seed density (m^{-2}) at both sites where seagrass was present (green) and sites where *Zostera spp* were absent (red).

3.9 Field observations

At all the study sites, personal observations recorded by the surveyors, indicated the risks to *Z. noltii* in the area. A number of the sites assessed had issues with disturbance, with physical damage inflicted by commercial cockling activities

and bait digging (Figure 25). 6 out of the 10 study sites where *Z. noltii* was present had boat anchoring or moorings present or in close proximity to the seagrass. Elevated nutrient levels were also observed at one of the sites through increased opportunistic macroalgae (Figure 26), effecting the water quality and light availability to *Z. noltii* at the site. Patches of *Z. noltii* bleaching were also noted at Angle Bay, although the causality was unknown (Figure 27).



Figure 25 Area of intensive bait digging to the north of the intertidal *Z. noltii* bed in Angle Bay. Source: authors own, 2016.



Figure 26 Opportunistic macroalgae observed at West Williamson, from extensive algae cover of the *Z. noltii* bed. Source: authors own, 2016



Figure 27 Observed *Z. noltii* bleaching at Angle Bay, where the causality is unknown. Source: authors own, 2016.

4.0 Discussion

Seagrass ecosystems are dynamic and ecologically important habitats that are in need of monitoring (Borum and Greve 2004). This study is the first quantitative assessment of both the distribution and health of *Z. noltii* populations along the South and West Wales coastline.

Although study sites such as the Pembroke dock could not be included, clear correlations with regards to changes in the extent of *Z. noltii* populations in the Milford Haven Waterway and Loughor estuary were observed. By revisiting historical sites, effort has been made to distinguish the difference between sites where *Z. noltii* is not present and sites where the data does not exist. The evaluation of a UAV as a seagrass mapping tool also highlights how this form of remote sensing can be used as an effective, novel method to mapping intertidal marine habitats.

4.1 Seagrass status and extent

Z. noltii populations in South and West Wales are currently increasing in spatial extent by 2% per year (Xha) over a x year period, with site specific regression and expansion patterns being observed. This finding is contrary to the large scale global patterns of decline (Waycott et al). Although current meadow expansion is clear this study also found x number of sites where seagrass has previously been recorded but now absent.

An overall increase in the mean rate of change (μ, yr^{-1}) indicates a significant expansion between the historical and current *Z. noltii* distributions, with the highest increase observed at the largest meadows. Similar increases in the size of intertidal *Z. noltii* meadows have been reported in other areas of western Europe (Table 12). Defining causality for these changes was beyond the scope of the present study however we provide a series of possible explanations for this, one of which is

improving water quality. The widespread decline in heavy industry may also be a contributing factor (Table x).

Table 12 European *Z. noltii* meadows, where expansion of the extent has been recorded in previous literature.

Location	Source	Most recent <i>Z. noltii</i> record	Total Surface Area (ha)	Mean % rate of change (yr ⁻¹)
Bourgneuf Bay, France	(Barille et al. 2009)	2009	586	13.0
De Keeg-De Ans, Dutch Wadden Sea	(Philippart and Dijkema 1995)	1987/1988	0.23	3.6
North Wadden Sea	(Reise and Kohlus 2008)	2006	10020	18.0
		Global Average	3535.41	11.53
		Study Results	73.27	2.09±20.78

The upper limits of the *Z. noltii* meadows (on the shore) remained almost unchanged, likely due to a threshold in which the negative effects of desiccation cannot be counteracted (Barille et al. 2009). The lower shore boundaries were observed to be expanding into the mid-intertidal zone. Inland migration was also observed and higher ZCI were observed for the expanding *Z. noltii* study sites.

Expanding meadows displayed a higher habitat health, with increased *Z. noltii* coverage, shoot density and canopy height. Elevated seed densities were also recorded at expanding meadows suggesting sites have a significantly higher resilience and therefore more likely to survive against potential threats (Unsworth et al, Maxwell et al). The observed gradual linear increase and good habitat condition indicate that the major Sea Empress oil spill of 1996 (Edwards and White 1998) did not significantly affect the long-term health and abundance of seagrass; confirmed by field observations (Moore 2006) and the spatial extent of the *Z. noltii* meadow.

Study sites such as Llanrhidian Sands and Sprinkle Pill displayed signs of regression most likely caused by changes in the substratum, from muddy sand in which seagrass can thrive in to areas of rippled sand in which *Zostera* is unable to grow (Mazik and Boyes 2009; Dolch and Reise 2010). Anthropogenic impacts

including activities such as intensive cockling in these small meadows is most likely to have disrupted the growth of *Z. noltii*. Reduced coverage, shoot density and canopy height was observed at these sites and repeated disturbance to the canopy is likely to have reduced the seed output and deplete the seedbank for future distributions (Unsworth *et al.* 2015). Vehicle's observed driving across the seagrass have led to further damage (Figure 27) and expansion of the *Z. noltii* extent was also potentially limited at the West Williamson study site, due to increase in *Ulva spp* cover most likely caused by DIN entering the waterway from nearby agricultural land (Natural Resources Wales 2016). This reduces the seagrass light availability and ability to photosynthesise. Similar small-scale declines have also been observed in the Dutch Wadden Sea (OSPAR 2009), due to increased density of lugworms resulting in younger shoots becoming smothered with sediment and intensive grazing of *Brenta bernicla*.

Table 13 Possible explanatory mechanisms for the expansion of *Z. noltii* at specific study sites (PE, AB, PW, PD and WW) from 2004. Adapted from Barille et al (2009).

Expansion Mechanism	Possible Outcomes	Observed Effects
Increased Light Availability	<ul style="list-style-type: none"> a) Tidal emersion patterns change, due to local accretion b) Turbidity of the water decreases. c) Reduced nutrient concentrations will limit periphyton on blades and increase light availability. 	<ul style="list-style-type: none"> a) Positive accretion observed by permanent cocklers at sites such as Penclacywdd. For sites that are expanding downwards such as Angle Bay it would justify the expansion, by improving the light conditions in the mid-intertidal zone as <i>Z. noltii</i> photosynthesise mainly at low tide. b) No data available. c) Nutrient levels were obtained for Milford Haven and displayed high levels associated to the sample areas. However, a slight decrease in the dissolved inorganic nitrate (DIN) and an overall increase in the dissolved inorganic phosphorus (DIP) has been noted in the last 14 years (Natural Resources Wales 2014). Regression analysis from the 5 largest sewage treatment works (STWs) in the Milford Haven waterway also indicate a downward trend, with only ~8% of the DIN load attributing from continuous point sources such as STW (Natural Resources Wales 2016) and that the water quality in the study area is in fact increasing.
Increase in temperature	<ul style="list-style-type: none"> a) Increases the rate of photosynthesis b) Shift in the <i>Z. noltii</i> distribution 	<ul style="list-style-type: none"> a) Sea surface temperatures are increasing (0.2°C/decade)(IPCC 2007), which increases the photosynthetic efficiency of PSII (Collier and Waycott 2014). Studies into the effects of higher temperatures on <i>Z. noltii</i> populations in Wales are limited and no effects were visibly observed. However, the relationship needs long term monitoring as higher temperatures could rise above the <i>Z. noltii</i> tolerance (approximately 38°C, sampled from populations in Ria Formosa), causing an increase in the synthesis of heat-shock proteins (HSP) (Massa <i>et al.</i> 2008) and negatively impacts the plant. b) Global <i>Z. noltii</i> distributions are shifting northwards (expected to move 888km towards the poles by the end of the 21st century) due to increased seawater temperatures (Valle <i>et al.</i> 2014). Although this is unlikely to influence the current distribution of <i>Z. noltii</i> in Wales could have a long-term impact on seagrass species in the UK.
Increase in Salinity	<ul style="list-style-type: none"> a) Allow rapid colonisation of <i>Z. noltii</i> in new areas 	<ul style="list-style-type: none"> b) No data available
Sea level rise (SLR)	<ul style="list-style-type: none"> a) Increasing the intertidal area available for <i>Z. noltii</i> growth. 	<ul style="list-style-type: none"> a) Observed at sites such as Garren Pill and Penclacywdd, where <i>Z. noltii</i> populations are moving further inland to.
Sediment becoming suitable	<ul style="list-style-type: none"> a) Decreased density of lugworms (<i>Arenicola marina</i>) that reduces the impact of bioturbation. b) Change in the content and firmness of the sediment. 	<ul style="list-style-type: none"> a) Little to none <i>A. marina</i> were observed in the field. Sites where more <i>A. marina</i> pits were observed such as Angle Bay, displayed reduced coverage, shoot density and canopy height. Lack of historical data and consistent seagrass monitoring in South and West Wales meant changes in <i>A. marina</i> distribution could not be analysed. b) Further scientific analysis is required to detect a historical change. The results of the GLM do indicate that sediment influences the habitat characteristics and previous studies reveal how the <i>Z. noltii</i> coverage and extent was positively related to the clay content of the sediment (Philippart and Dijkema 1995). Clay layers provide a firm rooting for the plant and prevent the settlement of lugworms (Reise and Kohlus 2008).
Reduction in relative exposure index	<ul style="list-style-type: none"> a) Increased shelter provides a more suitable area for <i>Z. noltii</i> to grow and survive 	<ul style="list-style-type: none"> c) Recent relative exposure index calculations reveal that sites in the Milford Haven Waterway have the lowest exposure in Wales (Brown 2015), supporting the expansion of <i>Z. noltii</i> meadows. Extensive coastal development in areas also increase local accretion making areas more suitable for <i>Z. noltii</i> growth.
Decrease in extreme weather events	<ul style="list-style-type: none"> a) Reduced drought effects will limit the impact on <i>Zostera</i> biomass and dynamics of species such as <i>H. ulvae</i> in the seagrass ecosystem. b) Decrease in storms, reduces wave energy and suspended sediment. 	<ul style="list-style-type: none"> a) Increased rainfall? Higher frequency of heat-waves has been recently recorded in the UK, opposing this theory. b)

Patchiness and further clumped distribution of *Z. noltii* was also mainly observed at sites declining in size or at the boundary and expanding meadows (Figure 29). Fragmentation can therefore be used as an identification of a disturbed meadow that is either in recovery or regressing after impact. It is generally caused by anthropogenic threats rather than a change in morphodynamics, leading to reduced ecosystem connectivity.

Furthermore, *Z. noltii* was found to be absent at many of the historical study sites (last surveyed before 1995) and in areas that display suitable environmental parameters in which *Zostera spp* can survive, disappearances likely due to extensive anthropogenic impacts. Limited baseline information from these sites limits the ability of this study to examine how much seagrass has been historically lost at these sites.

14



Figure 2815 Tractor marks observed at *Zostera* meadow in Porthdinllaen (North Wales). Source: Benjamin Jones, 2016.

Many ??? Study sites lacked *Z. noltii* seedbanks and this is most likely due to the *Zostera* seeds being heavy and negatively buoyant, therefore estimates of seed dispersal suggest that the seeds only have the ability to move a few metres and

despite the geophysical process the seeds rapidly settle, becoming incorporated into the sediment (Orth *et al.* 1994). However, other studies consider long distance dispersal (occurring over 10s of kilometres) as bare seeds, detached spathes and whole flowering shoots and that the absence of *Z. noltii* seeds at study sites could instead be due to low viability and successful germination levels within the seedbank. *Z. noltii* seed densities calculated within this study were much lower than those recorded in the literature (Table 14). This is most likely due to the effects of seasonality as *Z. noltii* forms new seeds at the end of August (Hootsmans *et al.* 1987), potentially reducing *Z. noltii* seed densities in the seedbank from June to July, when a high majority of the sampling for this study took place. The present studies are the first to examine *Z. noltii* seeds in the UK reflecting the limited understanding of seagrass reproduction in the region. Further research into changes into *Z. noltii* reproduction and seedbanks are needed to help understand the resilience of these meadows (Box 1.0) .

Table 14 Estimates of *Z.noltii* seed density recorded in previous literature. Adapted from Zipperle *et al.* (2009).

Location	Source	Year of fieldwork	Estimated Seed density in sediment (m ⁻²)
Konigshafen Bay, Island of Sylt, German Wadden Sea	(Zipperle <i>et al.</i> 2009)	2004	487.5±269.4
		2005	367.3±95.5
Zandkreek, The Netherlands	(Harrison 1993)	1989-1990	157±45.8
	(Hootsmans <i>et al.</i> 1987)	1983	0-150
Ria Formosa Lagoon, Portugal	(Alexandre <i>et al.</i> 2006)	2003	312.1±66
Global Average			279.78±119.2
Study Average			1.4±2.1

Box 1.0 Future studies into the *Z. noltii* seedbank

The expansion of a *Z. noltii* meadow in theory should cause an increase in the viable seed density and the different type of seeds in the age structured seed bank could be used to indicate the historical distribution of a *Z. noltii* bed, based on the number of long-term seeds (<5yr) as oppose to the transient seeds (persisting for <1 year) (Thompson et al). The strong negative impacts of heat-stress on the seeds also means that the studies into the environmental factors that influence the *Z. noltii* seedbank and distribution of the seagrass populations can take place. However, previous resources display that only 12% of the seeds germinate in the field and survive to the seedling stage, therefore the quantity of the *Z. noltii* seeds is not representative of the size of the meadows. The origin of any seeds that germinate also cannot be assumed to be from a specific meadow without genetic analysis, as previous studies in the Wadden Sea display how 70% of the annual recruitment originated from outside the existing meadow or were seeds produced within the meadow boundary before 2002.

4.3 Affectability of drones as an alternative seagrass monitoring platform

The drone based mapping acted as an effective mapping tool, enabling wider spatial and temporal distributions of the dynamic seagrass ecosystem to be recorded. Many of the advantages to using a drone were addressed in section 1.4, with the time taken to capture the aerial data significantly lower than that when using other methods due to the facility to rapidly deploy and acquire data (Lomax *et al.* 2005) (previously displayed in Table 8). This is key in image acquisition, with cloudy conditions typical of the UK climate, limiting optical remote sensing techniques in previous studies. Instead the UAV can be kept in a state of readiness and only be deployed in suitable atmospheric conditions, reducing the time taken to complete *Z. noltii* surveys accurately.

There are limitations to using a UAV for seagrass mapping, such as the lightweight nature making it more susceptible to wind and turbulence in comparison to conventional aerial photography, leading to potential distortion of the aerial data (Peterson *et al.* 2003) (Figure 28). This posed a significant problem at exposed study

sites in the Loughor Estuary, however other forms of remote sensing such as using kites as an aerial platform are being investigated in these areas (Duffy and Anderson 2016). The operator skills may have also influenced the altitude and flight trajectory, with a more experienced pilots producing more comprehensive and consistent images compared novel UAV operators (Dugdale 2007). Furthermore, the large aerial image dataset provided from the UAV data may also reduce the time-efficiency of using a drone with the post-processing and generation of an orthomosaic proving both difficult and time consuming. However, despite these disadvantages the use of drone-based surveys is still recommended.

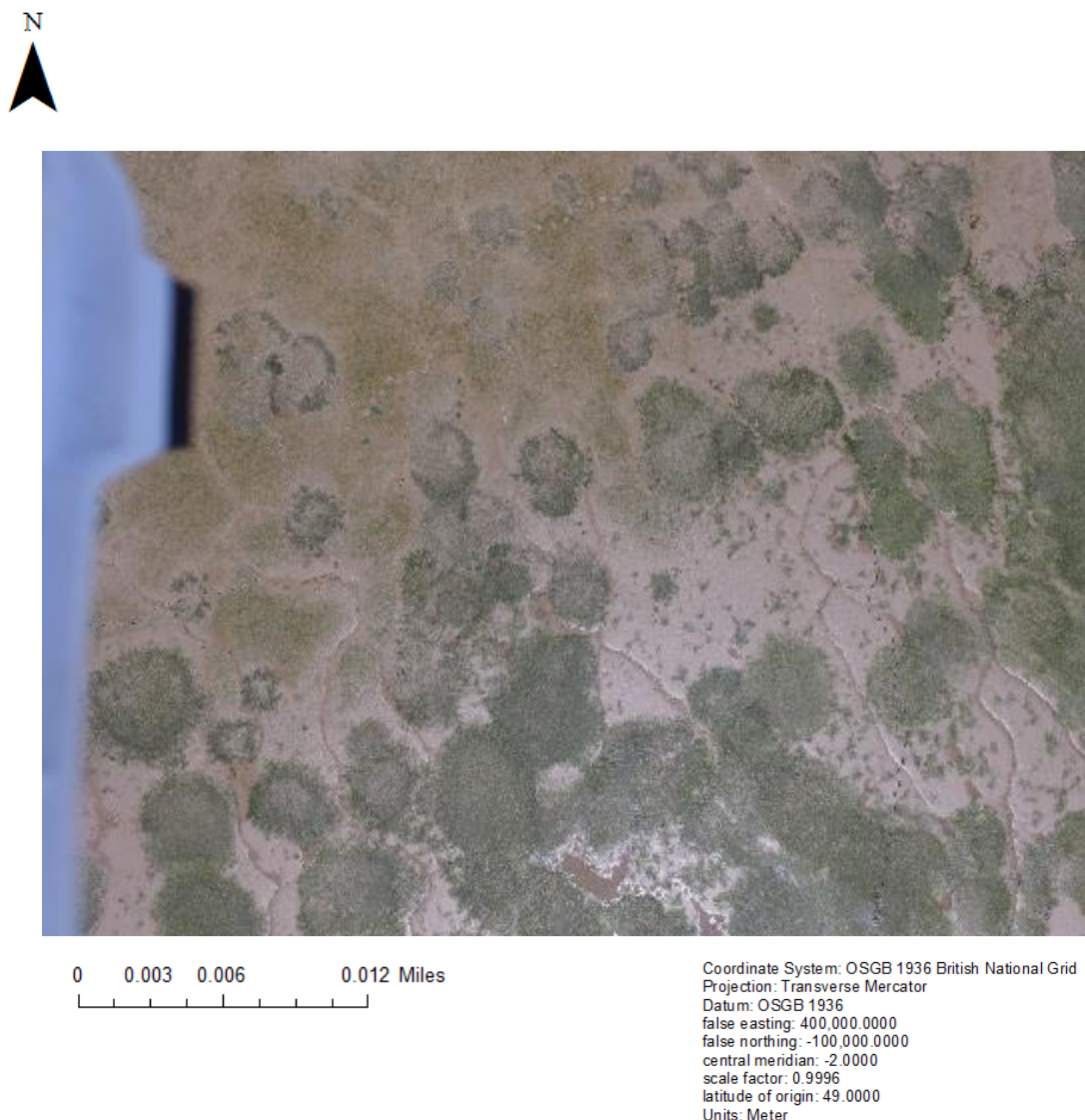


Figure 29 Aerial data recorded at Pwllcrochan, July 2016, displaying clear patchiness along the meadow boundary, most likely caused by Strong winds also led to the model (DJI Phantom 3 Professional) blocking part of the photograph. Source: Authors own, 2016.

Classifications of the aerial data need further development, with the sensitivity of the mapping often being restricted and not detecting areas low density *Z. noltii* (Valle et al. 2015). Biological information such as seagrass morphometric measurements and above-ground biomass, can also be derived from the NDVI and used to detect changes in *Z. noltii* distribution. Although the NDVI calculated in this study is not deemed as true (due to a lack of calibration with the targets present in the aerial data) values obtained matched those calculated in previous studies (Table 15). However, NDVI must be applied with caution as due to high influences of sediment background in estuarine conditions (Bargain *et al.* 2012).

Table 15 The decision rules used to classify *Z. noltii* beds that had previously been remotely sensed with SPOT multispectral images. Source: Barille et al, 2010.

NDVI Range	Description
-1 to 0	Turbid water and bare sediment.
0 - 0.2	Sediment with microphytobenthos and/or low <i>Z. noltii</i> cover.
0.2 – 0.7	<i>Z. noltii</i> with biomass variations

Box 2.0 Potential developments for the use of a UAV in *Z. noltii* mapping

The use of a UAV offers the potential for long-term studies to evaluate topographic changes in the seagrass ecosystem. Short term surveys studying seasonality as well as longer time-series analysis could be used to assess how environmental parameters such as elevation change through both orthomosaics and digital elevation models (DEM). Photogrammetric DEMs over time, would allow differences in DEM's to be computed, illustrating erosion or accretions at specific study sites as displayed by studies into mudflat morphodynamics by Jaud et al (2016) (Figure). Differences in elevation and topographical features can also be used to enhance orthomosaic classification accuracy (Chust *et al.* 2010) due to strong association between *Z. noltii*, estuarine habitat and terrain levels. Furthermore, analysis into the use of a UAV in calculating leaf area index (LAI) would allow calculations into the extent of photosynthesising tissue to take place (Yang and Yang 2009; Wicaksono and Hafizt 2013).

4.5 Conclusion

Z. noltii populations in South and West Wales are currently expanding, but evidence exists of potentially extensive historic loss throughout the last 50 years., with changes dependent on both site level environmental factors and anthropogenic threats. A lack of current consistent monitoring surveys limits knowledge of *Z. noltii* distribution. Monitoring programs need to be put in place and should be based on the methods used in this study. Future UAV seagrass monitoring should take place in September to encompass the maximum amount of above-ground biomass that can be sampled and remotely sensed. Seagrass coverage, shoot density and canopy height should be used to monitor the health *Z. noltii* populations and if financially viable, parameters such as molar C:N and C:P ratios should be calculated to provide a true indication of environmental status (Jones and Unsworth 2016). Consistent monitoring other intertidal environments such as saltmarsh and mussel crumble extent will also help to identify the areas that have the potential for *Z. noltii* colonisation (Mazik and Boyes 2009; Howson 2012).

5.0 Acknowledgements

First and foremost, I would like to thank all the kind volunteers for all their assistance with the sampling of this study. I would like to thank Leanne Cullen-Unsworth, Richard Unsworth, Richard Lilley and Benjamin Jones (Project Seagrass) for all the guidance and support with my project. I would also like to offer my gratitude to James P Duffy (University of Exeter) for all the knowledge and assistance in the field regarding the drone data collection. Finally, I would like to thank my family for their support.

6.0 References

- AgiSoft, L. (2015). Agisoft PhotoScan Professional Edition, Version 1.2.0. <http://www.agisoft.com/downloads/installer/>.
- Alexandre, A., Cabaco, S., Santos, R. and Serrao, E. A. (2006). Timing and success of reproductive stages in the seagrass *Zostera noltii*. *Aquatic Botany* **85**:219-223.
- Anderson, K. and Gaston, K. J. (2013). Lightweight unmanned aerial vehicles will revolutionize spatial ecology. *Frontiers in Ecology and the Environment* **11**:138-146.
- Armstrong, R. A. (1993). Remote sensing of submerged vegetation canopies for biomass estimation. *Int. J. Remote Sensing* **14**:621-627.
- Bargain, A., Robin, M., Le Men, E., Huete, A. and Barille, L. (2012). Spectral response of the seagrass *Zostera noltii* with different sediment backgrounds. *Aquatic Botany* **98**:45-56.
- Barille, L., Robin, M., Harin, N., Bargain, A. and Launeau, P. (2009). Increase in seagrass distribution at Bourgneuf Bay (France) detected by spatial remote sensing *Aquatic Botany*.
- Bertelli, C. M. and Unsworth, R. K. F. (2014). Protecting the hand that feeds us: Seagrass (*Zostera marina*) serves as commercial juvenile fish habitat. *Marine Pollution Bulletin* **83**:425-429.
- Bhattacharya, B., Sarkar, S. K. and Das, R. (2003). Seasonal variations and inherent variability of selenium in marine biota of a tropical wetland ecosystem: implications for bioindicator species. *Ecological Indicators* **2**:367-375.
- Borum, J. and Greve, T. M. (2004). The four European seagrass species. In: Borum, J. and Duarte, C.M. and Krause-Jensen, D. and Greve, T.M. (eds.) *European Seagrasses: An Introduction to Monitoring and Management*. . The M&MS Project, pp. 1-7.
- Brown, G. D. (2015). Modelling the potential distribution of *Zostera marina* in Wales. Degree of Master of Science in Environmental Biology; Conservation and Resource management (MSc) Thesis, Swansea University 2015.
- Bunker, F. S. D. (2008). Intertidal SAC monitoring *Zostera noltii* in Angle Bay, Pembrokeshire Marine SAC 2008 CCW Marine Monitoring Report No: 81, 51pp + ix, Countryside Council for Wales, Bangor.
- Carr, M. H., Neigel, J. E., Estes, J. A., Andelman, S., Warner, R. R. and Largier, J. L. (2003). Comparing marine and terrestrial ecosystems: implications for the design of coastal marine reserves. *Ecological Applications* **13**:S90-S107.

Casella, E., Rovere, A., Pedroncini, A., Stark, C. P., Casella, M. and Ferrari, M. (2016). Drones as tools for monitoring beach topography changes in the Ligurian Sea (NW Mediterranean). *Geo-Marine Letters* **36**:151-163.

Charpentier, A., Grillas, P., Lescuyer, F., Coulet, E. and Auby, I. (2005). Spatio-temporal dynamics of a *Zostera noltii* dominated community over a period of fluctuating salinity in a shallow lagoon, Southern France *Estuarine, Coastal and Shelf Science* **64**:307-315.

Chust, G., Grande, M., Galparsoro, I., Uriarte, A. and Borja, A. (2010). Capabilities of the bathymetric Hawk Eye LiDAR for coastal habitat mapping: a case study within a Basque estuary. *Estuarine Coastal and Shelf Science* **78**:633-643.

Collier, C. J. and Waycott, M. (2014). Temperature extremes reduce seagrass growth and induce mortality. *Marine Pollution Bulletin* **83**:483-490.

Coyer, J. A., Hoarau, G., Kuo, J., Tronholm, A., Veldsink, J. and Olsen, J. L. (2013). Phylogeny and temporal divergence of the seagrass family zosteraceae using one nuclear and three chloroplast loci. *Systematics and Biodiversity* **11**.

Cunha, A. H. and Araujo, A. (2009). New distribution limits of seagrass beds in West Africa. *Journal of Biogeography* **36**:1621-1622.

Davison, D. M. and Hughes, D. J. (1998). *Zostera* Biotopes (volume I) An overview of dynamics and sensitivity characteristics for conservation management of marine SACs. Scottish Association for Marine Science (UK Marine SACs Project).

den Hartog, C. (1970). The sea-grasses of the World. *Verhandelingen Der Koninklijke Nederlandse Akademie Van Wetenschappen, AFD. Natuurkunde* **59**.

Dolch, T. and Reise, K. (2010). Long-term displacement of intertidal seagrass and mussel beds by expanding sandy bedforms in the northern Wadden Sea. *Journal of Sea Research* **63**:93-101.

Duffy, J. P. and Anderson, K. (2016). A 21st-century renaissance of kites as platforms for proximal sensing. *Progress in Physical Geography* **40**:352-361.

Dugdale, S. J. (2007). An evaluation of imagery from an unmanned aerial vehicle (UAV) for the mapping of intertidal macroalgae on Seal Sands, Tees Estuary, UK, Durham theses, Durham University. Available at Durham E-Theses Online: <http://etheses.dur.ac.uk/2879/>.

Duggan-Edwards, M. and Brazier, D. P. (2015). Intertidal SAC monitoring *Zostera noltii* in Angle Bay, Pembrokeshire Marine SAC 2013 NRW Evidence Report No: 55, 38pp +xi, Natural Resources Wales, Bangor

Edwards, R. and White, I. (1998). The Sea Empress oil spill. Terance Dalton, Lavenham, Suffolk.

- Grech, A. and Coles, R. G. (2010). An ecosystem-scale predictive model of coastal seagrass distribution. *Aquatic Conservation: Marine and Freshwater Ecosystems* **20**:437-444.
- Green, E. P. and Short, F. T. (2003). World Atlas of Seagrasses (Copub: Unep-Wcmc). University of California Press.
- Harrison, P. G. (1993). Variations in demography of *Zostera marina* and *Z. noltii* on an intertidal gradient. *Aquatic Botany* **45**:63-77.
- Hodges, J. and Howe, M. (2007). Milford Haven Waterway Monitoring of Eelgrass, *Zostera noltei*, following the Sea Empress Oil Spill.
- Hootsmans, M. J. M., Vermaat, J. E. and Van Vierssen, W. (1987). Seed-bank development, germination and early seedling survival of two seagrass species from The Netherlands: *Zostera marina* L. and *Zostera noltii* hornem. *Aquatic Botany* **28**:275-285.
- Howson, C. M. (2012). Intertidal SAC monitoring, Carmarthen Bay SAC, September 2009. CCW Marine Monitoring Report No. 79, 147pp + x, Countryside Council for Wales, Bangor. .
- IPCC. (2007). Climate Change 2007: The Physical Science Basis. Summary for Policymakers: 1-21.
- Jackson, E. L., Higgs, S., Allsop, T., A, C., Evans, J. and Langmead, O. (2011). Isles of Scilly Seagrass Mapping. Natural England Commissioned Reports, Number 087.
- Jaud, M., Grasso, F., Le Dantec, N., Verney, R., Delacourt, C., Ammann, J., Deloffre, J. *et al.* (2016). Potential of UAV's for Monitoring Mudflat Morphodynamics (Application to the Seine Estuary, France). *ISPRS Int. J. Geo-Inf.* **5**:20.
- Johnson, L. and Gage, S. (1997). Landscape approaches to the analysis of aquatic ecosystems. *Freshwater Biology* **37**:113-132.
- Jones, B. L. and Unsworth, R. K. F. (2016). The perilous state of seagrass in the British Isles. *R. Soc. open sci* **3**.
- Kay, Q. (1998). A review of the existing state of knowledge of the ecology and distribution of seagrass beds around the coast of Wales. Report to the Countryside Council for Wales.
- Knudby, A. and Nordlund, L. (2011). Remote sensing of seagrasses in a patchy multi-species environment. *International Journal of Remote Sensing* **32**.

Koedsin, W., Intararuang, W., Ritchie, R. J. and Huete, A. (2016). An Integrated Field and Remote Sensing Method for Mapping Seagrass Species, Cover, and Biomass in Southern Thailand *Remote Sensing* **8**.

Krause-Jensen, D., Quaresma, A. L., Cunha, A. H. and Greve, T. M. (2004). How are seagrass distribution and abundance monitored? In: Borum, J. and Duarte, C.M. and Krause-Jensen, D. (eds.) *European Seagrasses: An introduction to Monitoring and Management*. pp. 45-53.

Lomax, A. S., Corso, W. and Etro, J. F. (2005). Employing Unmanned Aerial Vehicles (UAVs) as an Element of the Integrated Ocean Observing System;. *Proceedings of the Marine Technology Society/IEEE* **1**:184-190.

Lyons, M., Phinn, S. and Roelfsema, C. (2011). Integrating Quickbird Multi-Spectral Satellite and Field Data: Mapping Bathymetry, Seagrass Cover, Seagrass Species and Change in Moreton Bay, Australia in 2004 and 2007. *Remote Sensing* **3**:42-64.

Maddock, A. (2011). UK Biodiversity Action Plan Priority Habitat Descriptions. Biodiversity Reporting and Information Group (BRIG), Joint Nature Conservation Committee.

Massa, S. I., Arnaud-Haond, S., Pearson, G. A. and Serrao, E. A. (2008). **Temperature tolerance and survival of intertidal populations of the seagrass *Zostera noltii* (Hornemann) in Southern Europe (Ria Formosa, Portugal)**. *Hydrobiologia* **619**:195-201.

Mazik, K. and Boyes, S. (2009). Intertidal monitoring of eelgrass *Zostera noltii* in the BurryInlet, Carmarthen Bay and Estuaries SAC. CCW Marine Monitoring Report No 53.

McEvoy, J. F., Hall, G. P. and McDonald, P. G. (2016). Evaluation of unmanned aerial vehicle shape, flight path and camera type for waterfowl surveys: disturbance effects and species recognition. *PeerJ* **4**.

McKenzie, L. J., Campbell, S. J. and Roder, C. A. (2003). Methods for Monitoring Seagrass Status. *Seagrass-Watch: Manual for Mapping & Monitoring Seagrass Resources by Community (citizen) volunteers*. 2nd ed. (QFS, NFC, Cairns), pp. 41-58.

Mckenzie, L. J., Campbell, S. J. and Roder, S. J. (2003). Methods for Monitoring seagrass conditions & resilience. *Seagrass-Watch: Manual for Mapping & Monitoring Seagrass Resources by Community (citizen) volunteers*. 2nd ed. (QFS, NFC, Cairns), pp. 59-74.

McKenzie, L. J., Collier, C. and Waycott, M. (2012). Reef Rescue Marine Monitoring Program - Inshore Seagrass, Annual Report for the sampling period 1st July 2010 - 31st May 2011. Fisheries Queensland, Cairns. 230pp.

McKenzie, L. J., Collier, C. and Waycott, M. (2014). Reef Resuce Marine Monitoring Program - Inshore Seagrass, Annual Report for the sampling period 1st July 2011 - 31st May 2012. TropWATER, James Cook University, Cairns. 176pp.

Mcleod, E., Chmura, G. L., Bouillon, S., Salm, R., Bjork, M., Duarte, C. M., Lovelock, C. E. *et al.* (2011). A blueprint for blue carbon: toward an improvement understanding of the role of vegetated coastal habitats in sequestering CO₂. *Frontiers in Ecology and the Environment* **9**:552-560.

McMahon, K., van Dijk, K.-J., Ruiz-Montoya, L., Kendrick, G. A., Krauss, S. L., Waycott, M., Verduin, J. *et al.* (2014). The movement ecology of seagrasses. *Proc. R. Soc. B* **281**.

Meyer, C. A. (2008). Application of remote sensing methods to assess the spatial extent of the seagrass resource in St. Joseph Sound and Clearwater Harbor, Florida, U.S.A Thesis Geography, University of South Florida.

Moore, J. J. (2006). State of the marine environment in SW Wales, 10 years after the *Sea Empress* oil spill. A report to the Countryside Council for Wales from Coastal Assessment, Liaison & Monitoring, Coshaston, Pembrokeshire. CCW Marine Monitoring Report No: 21. 30pp.

Natural Resources Wales. (2014). Environmental Pressures on the Milford Haven Waterway, Report Reference A&R/SW/14/1.

Natural Resources Wales. (2016). Review of the Trophic Status of the Milford Haven Waterway.

Nikitik, C. (2015). Pembroke Environmental Monitoring Intertidal Eelgrass Report 2014, Report No: JUKL/B1810700/R29.

Orth, R. J., Luckenbach, M. and Moore, K. A. (1994). Seed Dispersal in a Marine Macrophyte: Implications for Colonization and Restoration. *Ecology* **75**:1927-1939.

OSPAR. (2009). Background Document for *Zostera* beds, Seagrass beds.

Paul, M. (2011). The role of *Zostera noltii* in wave attenuation. Thesis University of Southampton.

Paul, M. and Amos, C. L. (2011). Spatial and seasonal variation in wave attenuation over *Zostera noltii* *Journal of Geophysical Research* **116**.

Pergent-Martini, C. and Pergent, G. (2000). Are marine phanerograms a valuable tool in the evaluation of marine trace-metal contamination: example of the Mediterranean sea? *International Journal of Environmental Pollution* **13**:126-147.

Peterson, D. L., Brass, J. A., Smith, W. H., Langford, G., Wegener, S., Dunagan, S., Hammer, P. *et al.* (2003). Platform options of free-flying satellites, UAVs or

the International Space Station for remote sensing assessment of the littoral zone. *International Journal of Remote Sensing* **24**:2875-2804.

Philippart, C. J. M. and Dijkema, K. S. (1995). Wax and wane of *Zostera noltii* Hornem. in the Dutch Wadden Sea. *Aquatic Botany* **49**:255-268.

R Core Team. (2013). R: A language and environment for statistical computing. R Foundation for Statistical Computing, Vienna, Austria. URL <http://www.R-project.org/>.

Rasheed, M. A., Thomas, R., Roelofs, A. J., Neil, K. M. and Kerville, S. P. (2003). Port Curtis and Rodds Bay seagrass and benthic macro-invertebrate community baseline survey. DPI Information Series QI03058 (DPI, Cairns).

Reise, K. and Kohlus, J. (2008). Seagrass recovery in the Northern Wadden Sea? *Helgol Mar Res* **62**:77–84.

Salita, J. T., Ekau, W. and Saint-Paul, U. (2003). Field evidence on the influence of seagrass landscapes on fish abundance in Bolinao, northern Philippines. *Marine Ecology Progress Series* **247**:183-195.

Seitz, S. M., Curless, B., Diebel, J., Scharstein, D. and Szeliski, R. (2006). A comparison and evaluation of multi-view stereo reconstruction algorithms. *Proceedings of the 2006 IEEE Computer Society Conference on Computer Vision and Pattern Recognition*. IEEE Computer Society, Washington, DC. pp. 519-528.

Short, F. T., Carruthers, T. J. R., Waycott, M., Kendrick, G. A., Fourqurean, J. W., Callabine, A., Kenworthy, W. J. *et al.* (2010). *Zostera noltii*. The IUCN Red List of Threatened Species 2010: e.T173361A6999224. <http://dx.doi.org/10.2305/IUCN.UK.2010-3.RLTS.T173361A6999224.en>. Downloaded on **01 June 2016**.

Short, F. T., Polidoro, D., Livingstone, S. R., Carpenter, K. E., Bandeira, S., Bujang, J. S., Calumpong, H. P. *et al.* (2011). Extinction risk assessment of the world's seagrass species. *Biological Conservation* **144**:1961–1971.

Stace, C. A. (1997). *New Flora of the British Isles*. Cambridge: Cambridge University Press.

Telesca, L., Belluscio, A., Criscoli, A., Ardizzone, G., Apostolaki, E. T., Fraschetti, S., Gristina, M. *et al.* (2015). Seagrass meadows (*Posidonia oceanica*) distribution and trajectories of change. *Sci Rep* **5**.

Tucker, C. J. (1979). Red and photographic infrared linear combinations for monitoring vegetation. *Remote Sensing of Environment* **8**:127-150.

Uhrin, A. V. and Townsend, P. A. (2016). Improved seagrass mapping using linear spectral unmixing of aerial photographs. *Estuarine, Coastal and Shelf Science* **171**:11-22.

Ullman, S. (1979). The interpretation of structure from motion. *Proceedings of the Royal Society B* **203**:405-426.

Unsworth, R. K. F., Collier, C. J., Waycott, M., McKenzie, L. J. and Cullen-Unsworth, L. C. (2015). A framework for the resilience of seagrass ecosystems. *Marine Pollution Bulletin* 13.

Valle, M., Chust, G., Del Campo, A., Wisz, M. S., Olsen, S. M., Gardmendia, J. M. and Borja, A. (2014). Projecting future distribution of the seagrass *Zostera noltii* under global warming and sea level rise. *Biological Conservation* **170**:74-85.

Valle, M., Pala, V., Lafon, V., Dehouck, A., Garmendia, J. M., Borja, A. and Chust, G. (2015). Mapping estuarine habitats using airborne hyperspectral imagery, with special focus on seagrass meadows. *Estuarine, Coastal and Shelf Science* **164**:433-442.

Ventura, D., Bruno, M., Lasinio, G. J., Belluscio, A. and Ardizzone, G. (2016). A low-cost drone based application for identifying and mapping of coastal fish nursery grounds. *Estuarine, Coastal and Shelf Science* **171**:85-98.

Wicaksono, P. and Hafizt, M. (2013). Mapping Seagrass from Space: Addressing the Complexity of Seagrass LAI Mapping. *European Journal of Remote Sensing* **46**:18-39.

Wilde, J. (2016). Influence of Habitat Health on Abundance and Diversity of Juvenile Fish Within Meadows of *Posidonia oceanica* and its implications for food security in the Eastern Aegean. Thesis Cardiff University.

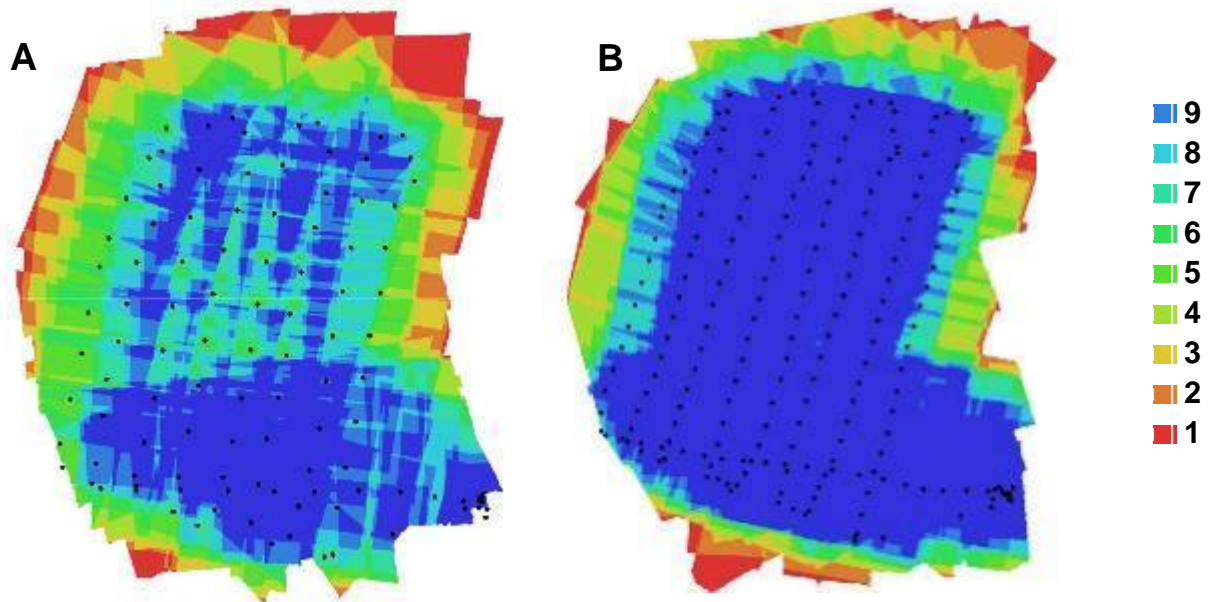
WWF. (2012). Historical changes in Welsh Seas: ecosystem trends. Online: In: CYMRU, W (ed.).

Yang, D. and Yang, C. (2009). Detection of Seagrass Distribution Changes from 1991 to 2006 in Xincun Bay, Hainan, with Satellite Remote Sensing. *Sensors* **9**:830-844.

Zar, J. H. (1984). *Biostatistical Analysis*. Sydney, Australia:Prentice Hall.

Zipperle, A. M., Coyer, J. A., Reise, K., Stam, W. T. and Olsen, J. L. (2009). Evidence for the persistent seed banks in dwarf eelgrass *Zostera noltii* in the German Wadden Sea. *Marine Ecology progress Series* **380**:73-80.

Appendix 1. Differences in the overlap and computed camera positions of images captured on the A) modified Xiaomi Yi Action and B) RICOH GR II consumer grade compact camera and Cameras.



Appendix 2. Image classification methods of UAV data

Unsupervised classifications

Referenced images were classified using an Iterative Self-Organising Data Analysis Technique (ISODATA). It is based on a k-means clustering algorithm, using multiple iterations to determine data grouping (Jensen, 2005) and no input is required from the surveyor. It was used as an initiation investigation to examine the number of significant classes in the composite image (bands 1-3), with the number of classes initially set larger than expected (30). The classes were then reduced through aggregation until up to 8 target classes remained (*Z. noltii* cover (2 levels), surface water, mud, rock, gravel, trees, fine algae, *Ulva spp*) depending on the individual study sites.

Supervised classifications

Supervised classifications use the knowledge of the surveyor to define spectral groups. Training areas were selected initially from the composite image using locations sampled during morphometric fieldwork, with extra areas added to ensure a wide variety of pixel types, locations and sizes were included, to generate a training signature. Images were then classified using the parametric (Jensen, 2005) Maximum Likelihood classification (MLC) which assess the variance of the training data with pixel brightness values (Meyer 2008). Points were grouped into similar target classes used in the unsupervised classification; *Z. noltii* (2 levels of coverage), microphytobenthos, rock/gravel, surface water and mud that were all identified through ground trothing.

Accuracy Assessments

Post-processing, accuracy assessments were performed on both the unsupervised and supervised raster layers to determining the success of the classification process. 30 random points were tested (to reflect the seagrass morphometric sampling), with the classification from the raw orthomosaic and unsupervised/supervised being compared. The overall accuracy was calculated from the error matrix generated and Cohen's Kappa calculation was then used to determine whether or not the results achieved by the classification were better than those strictly achieved by chance;

$$K = \frac{P_O - P_E}{1 - P_E}$$

Appendix 3. Error Matrices generated from unsupervised classifications of a) Pwllcrochan and b) Garren Pill.

Pwllcrochan

	Rock/Gravel	Surface Water	Dense <i>Z. noltii</i>	Medium density <i>Z. noltii</i>	Sparse <i>Z. noltii</i> /microphytobenthos	Mud
Rock/Gravel	0	0	0	0	0	1
Surface Water	0	1	0	0	0	0
Dense <i>Z. noltii</i>	0	0	1	0	0	0
Medium density <i>Z. noltii</i>	0	0	1	5	2	0
Sparse <i>Z. noltii</i> /microphytobenthos	0	0	2	3	6	1
Mud	0	2	0	0	2	2

Overall Accuracy = 50%

Kappa coefficient = 0.33

Garren Pill

	Dense <i>Z. noltii</i>	Trees	Medium <i>Z. noltii</i>	Sparse <i>Z. noltii</i> /microphytobenthos	Surface Water	Mud	Ulva spp
Dense <i>Z. noltii</i>	5	0	0	0	0	0	0
Trees	0	0	0	0	0	0	0
Medium <i>Z. noltii</i>	1	0	2	0	0	0	0
Sparse <i>Z. noltii</i> /microphytobenthos	2	0	1	0	0	1	0
Surface Water	0	0	0	0	2	1	0
Mud	0	0	2	1	4	8	0
Ulva spp	0	0	0	0	0	0	0

Overall Accuracy = 56.7%

Kappa Coefficient = 0.42

Appendix 4. Error Matrices generated from supervised classifications of a) Pwllcrochan and b) Garren Pill.

Pwllcrochan

	Dense Z. <i>noltii</i>	Medium Dense Z. <i>noltii</i>	Sparse Z. <i>noltii</i>	Mud	Dense Microphytobenthos	Sparse Microphytobenthos	Rock/Gravel	Surface Water
Dense <i>Z. noltii</i>	3	3	0	0	0	0	0	0
Medium Dense <i>Z. noltii</i>	2	6	0	0	0	0	0	0
Sparse <i>Z. noltii</i>	0	2	0	1	0	0	0	0
Mud	0	0	0	7	0	0	0	0
Dense Microphytobenthos	0	0	0	0	0	1	0	0
Sparse Microphytobenthos	0	0	0	0	0	1	0	0
Rock/Gravel	0	0	0	2	0	0	1	0
Surface Water	0	0	0	0	0	0	0	0

Overall Accuracy = 60%

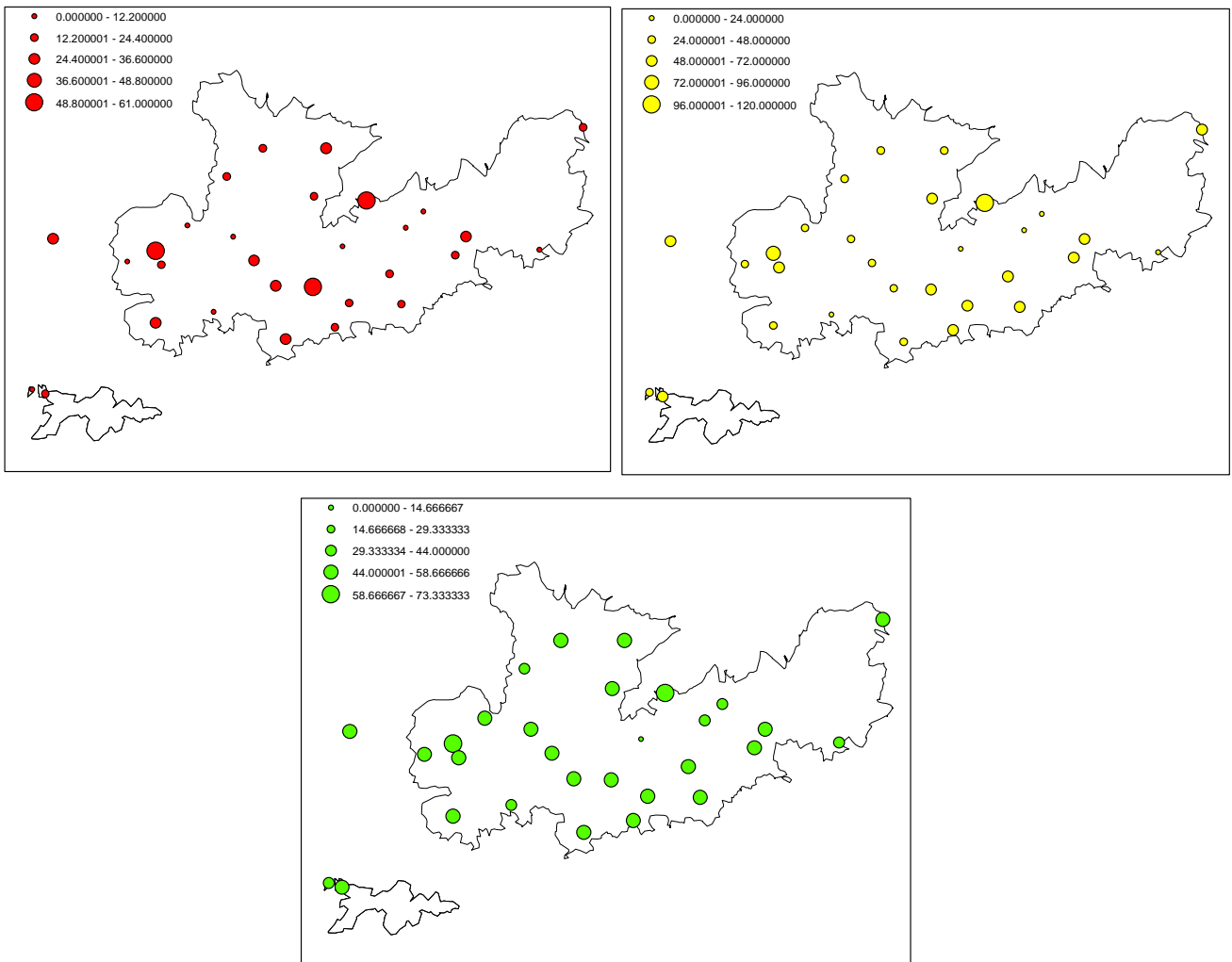
Kappa Coefficient = 0.48

Garren Pill

NEED TO COMPLETE

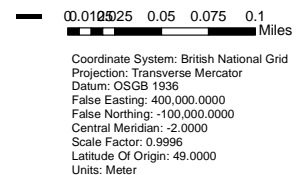
Appendix 5. Relationship between the seagrass morphometric values and spatial heterogeneity across the *Z. noltii* meadows. For Study sites LS1, LS2, LS3 and SP changes in habitat characteristics were not measured, due to the extremely small size of the site.

Site: PE



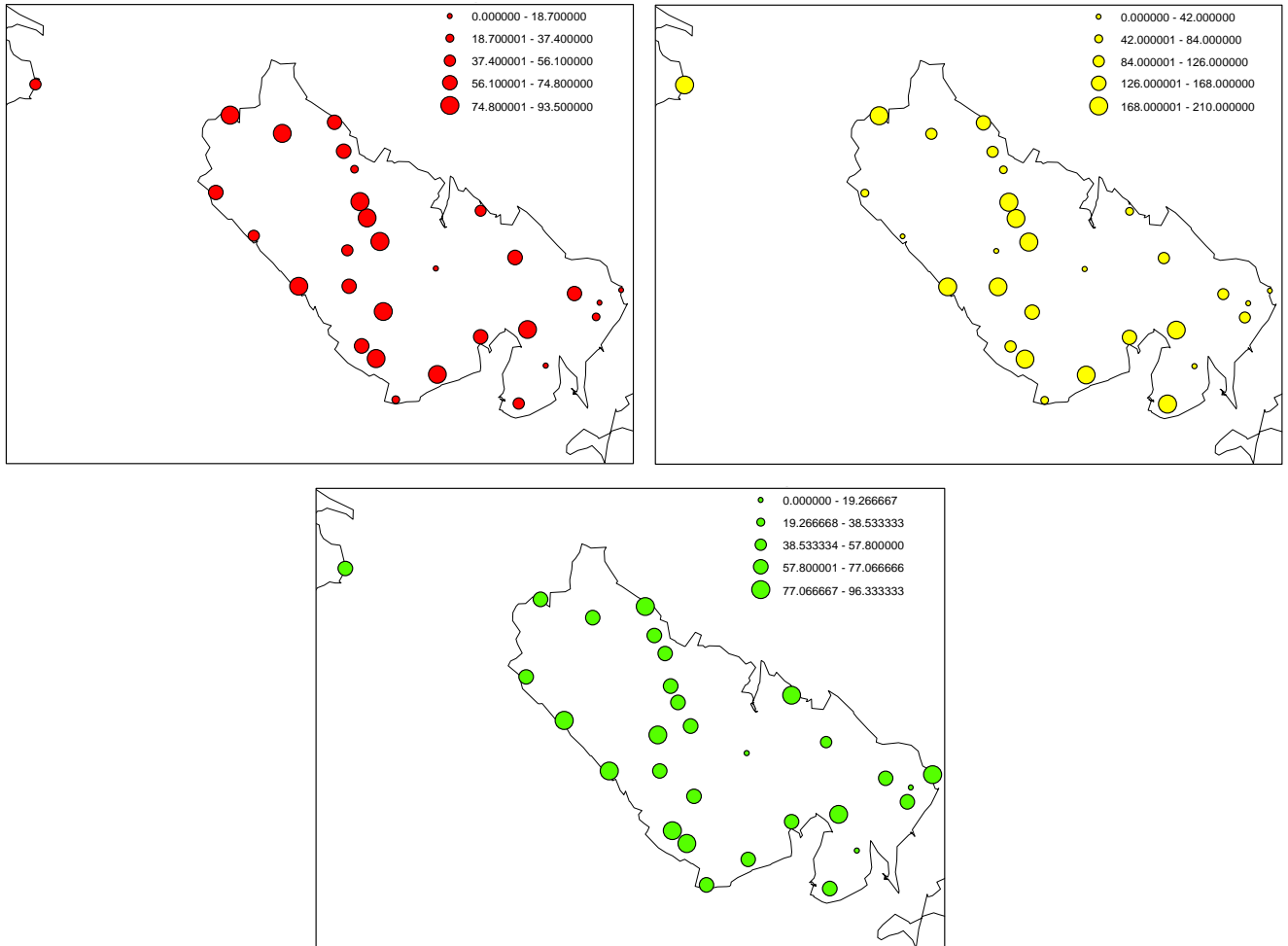
Legend

- = *Z. noltii* % cover
- = Seed density
- = Canopy height
- = Meadow boundary



Site:AB

Site: PW

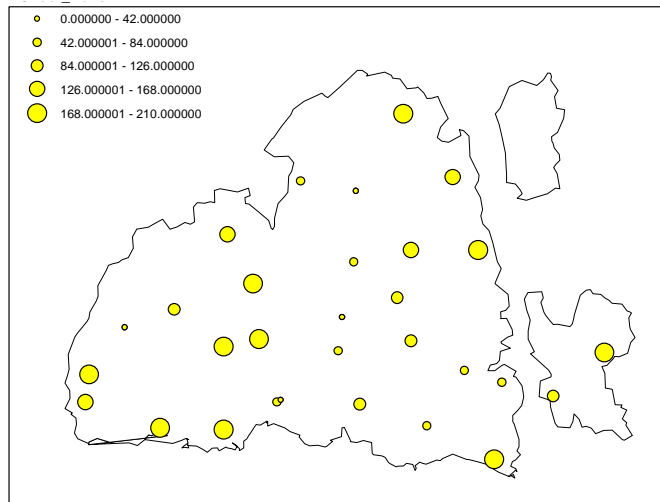
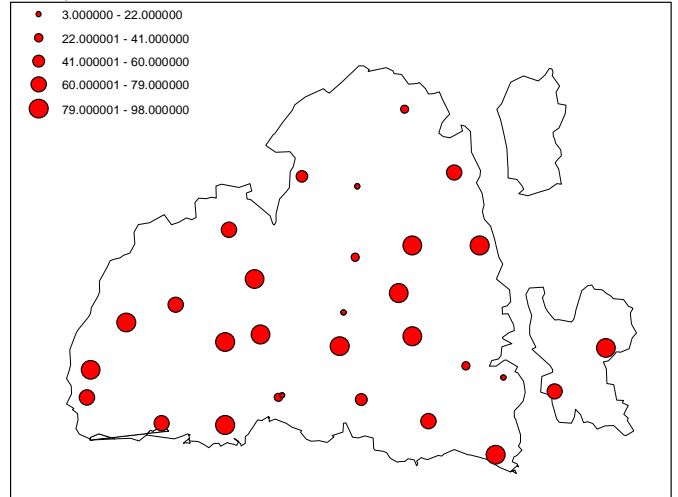
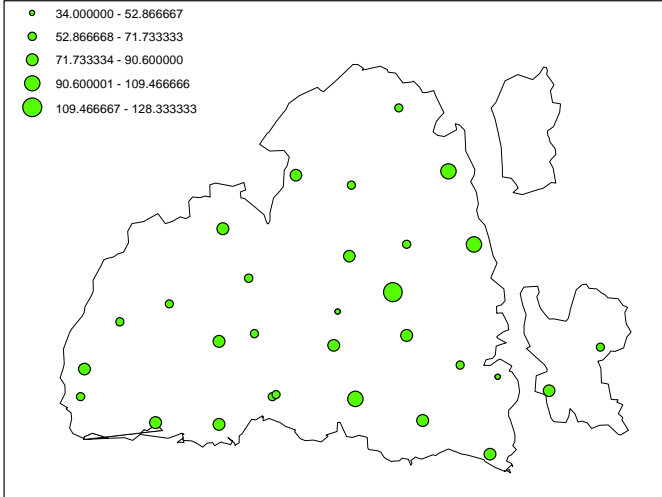


Legend

- *noltii* % cover
- seed density
- canopy height
- meadow boundary

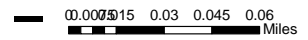
Coordinate System: British National Grid
 Projection: Transverse Mercator
 Datum: OSGB 1936
 False Easting: 400,000.0000
 False Northing: -100,000.0000
 Central Meridian: -2.0000
 Scale Factor: 0.9996
 Latitude Of Origin: 49.0000
 Units: Meter

Site: PD



Legend

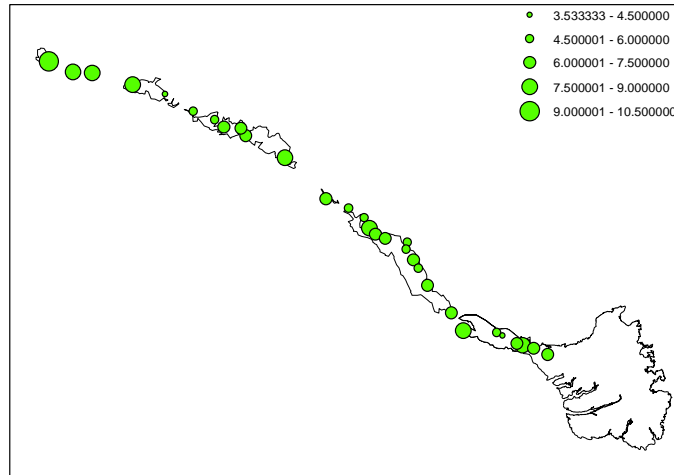
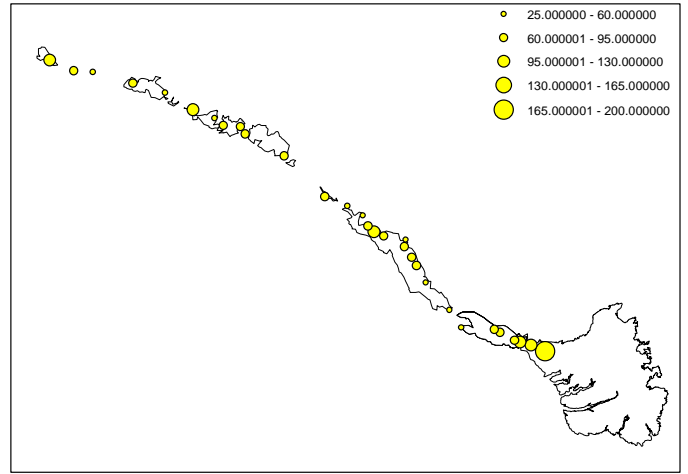
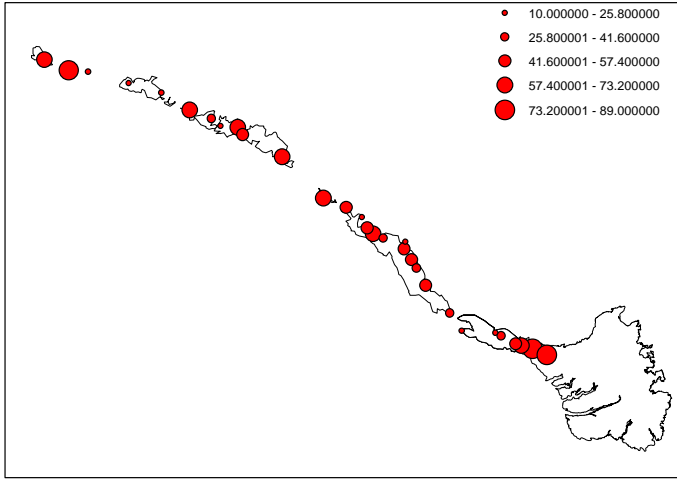
- = *Z. noltii* % cover
- = Seed density
- = Canopy height
- = Meadow boundary



Coordinate System: British National Grid
 Projection: Transverse Mercator
 Datum: OSGB 1936
 False Easting: 400,000.0000
 False Northing: -100,000.0000
 Central Meridian: -2.0000
 Scale Factor: 0.9996
 Latitude Of Origin: 49.0000
 Units: Meter

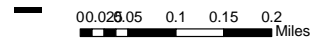
Site: WW

Site: GP



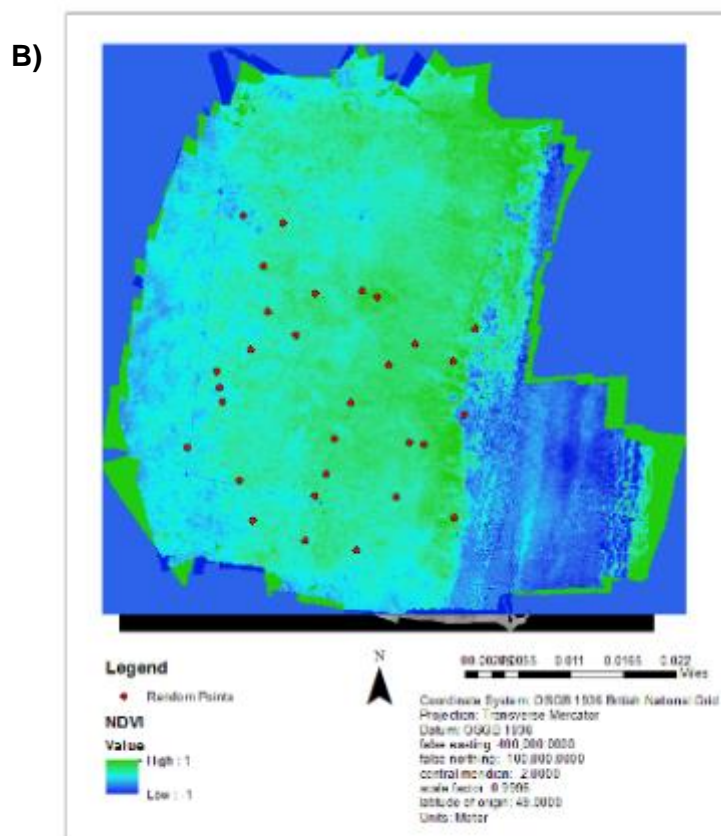
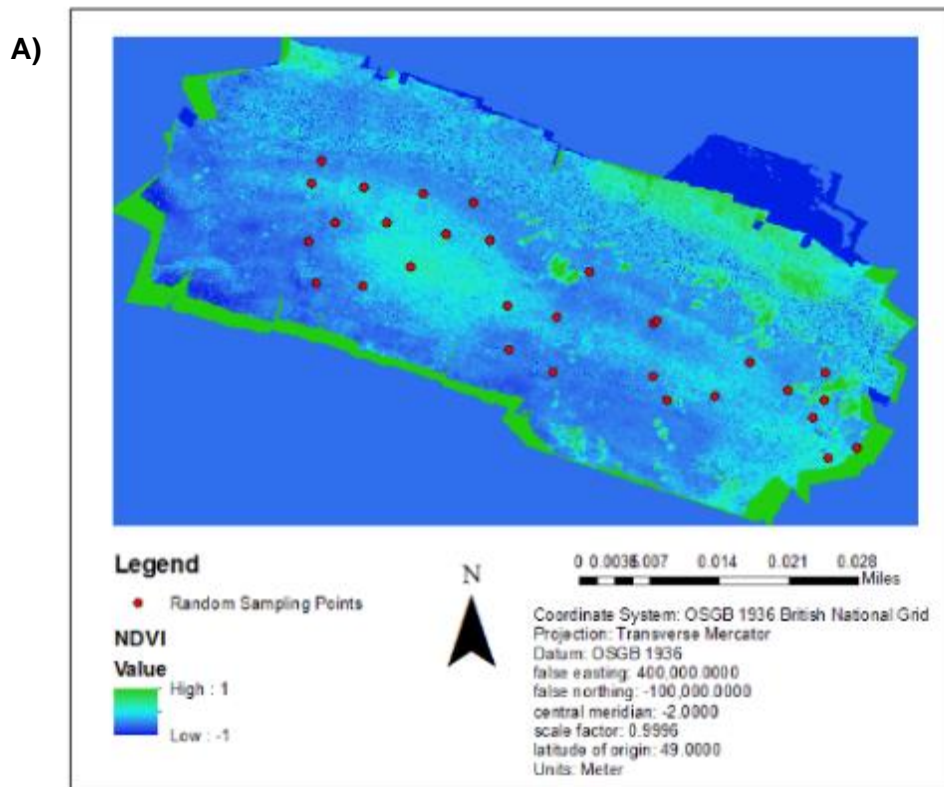
Legend

- = *Z. noltii* % cover
- = Seed density
- = Canopy height
- = Meadow boundary



Coordinate System: British National Grid
Projection: Transverse Mercator
Datum: OSGB 1936
False Easting: 400,000.0000
False Northing: -100,000.0000
Central Meridian: -2.0000
Scale Factor: 0.9996
Latitude Of Origin: 49.0000
Units: Meter

Appendix 6. Random morphometric sampling points superimposed on relative NDVI maps. Maps were generated from fine scale (15m) true-colour and NIR imagery at A) Garren Pill and B) Angle Bay, taken using a modified Xiaomi Yi Action Cameras. Source: L, Pratt, ArcMap 10.2.2, 2016.



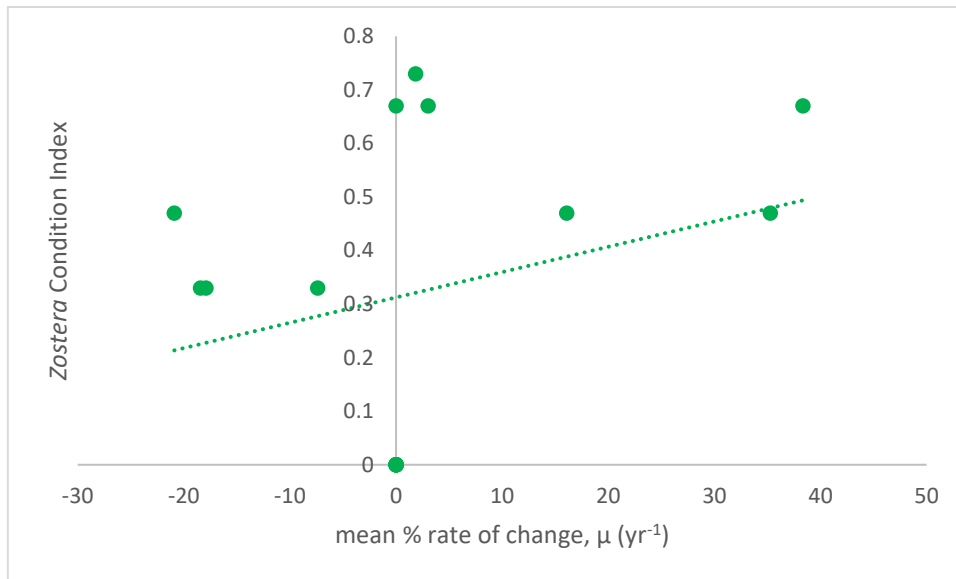
Appendix 7. Average Principal Components scores for each of the study sites.

Study Site	PC1	PC2
Llanrhidian Sands 1 (LS1)	-56.05	5.085667
Llanrhidian Sands 2 (LS2)	-52.3467	-10.7057
Llanrhidian Sands 3 (LS3)	-60.4	-20.17
Penclacwydd (PE)	-21.6323	8.189967
Angle Bay (AB)	-2.56933	13.55533
Pwllcrochan (PW)	59.6869	5.862333
Pembroke Dock (PD)	64.91467	-1.335
West Williamson (WW)	75.74333	-4.33413
Garren Pill (GP)	17.89367	-3.56227
Sprinkle Pill (SP)	-25.1843	7.466867

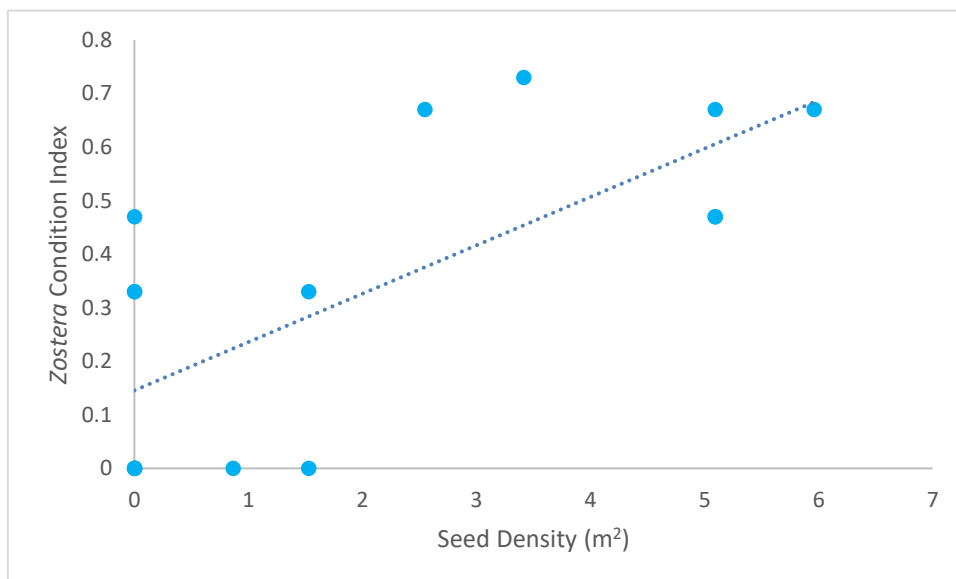
Appendix 8. Results of the *Z. noltii* morphometric GLM

	<i>Z. noltii</i> cover (%)	Shoot density (per/0.2m ²)	Leaf Length (mm)
Intercept	0.0432*	0.909	0.132
<i>Z. noltii</i> Cover	X	<0.000000225*	0.000132*
Shoot Density	<0.000000225*	X	0.298
Canopy Height	0.000132*	0.298	X
Seasonality	0.989	0.611	0.527
Sediment			
- Mud			
- Mud/Rock	0.0205*	0.733	0.492
- Mud/Sand	0.03498*	0.385	0.588
- Muddy Sand	<0.000000225*	0.450	0.608
Elevation	0.915	0.523	0.542

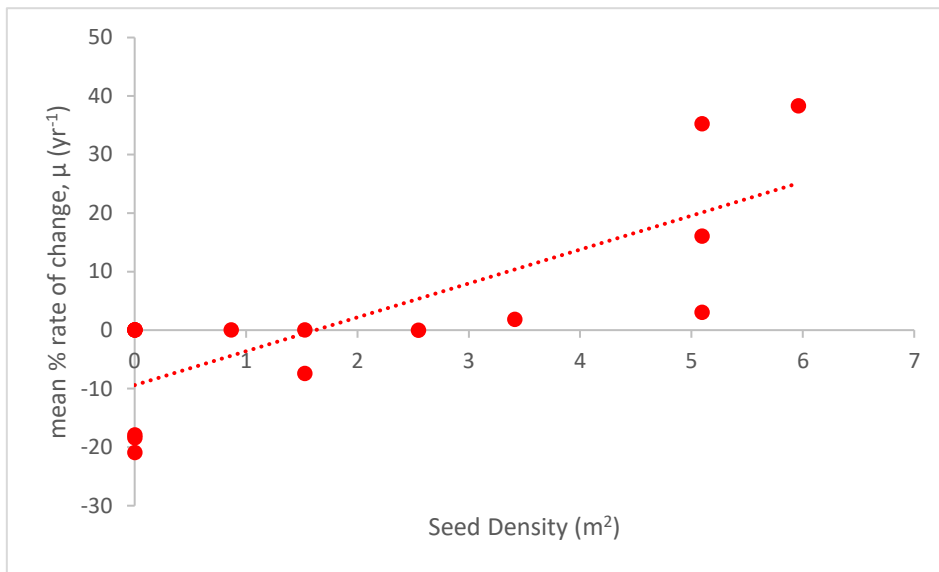
Appendix 9. Relationship between the mean rate of change in seagrass extent and the calculated *Zostera* Condition Index (ZCI) observed across 11 study sites along the South and West Wales coastline.



Appendix 10. Relationship between *Z. noltii* seed density and the calculated *Zostera* Condition Index (ZCI) observed across 11 study sites along the South and West Wales coastline.



Appendix 11. Relationship between *Z. noltii* seed density and the mean rate of change in seagrass extent observed across 11 study sites along the South and West Wales coastline.



Appendix 12. Relationship between *Z. noltii* seed density and the elevation of the seagrass meadows.

